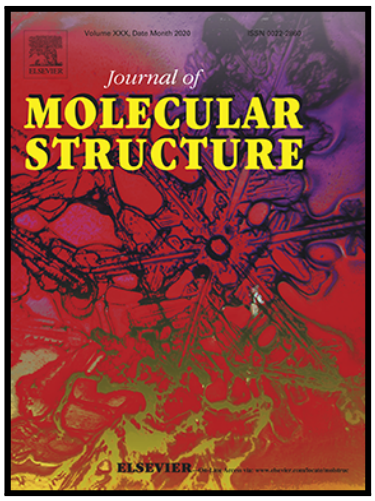

Design, Synthesis, in vitro and in silico evaluation of new 3-phenyl-4,5-dihydroisoxazole-5-carboxamides active against drug-resistant Mycobacterium tuberculosis

Nikhil Baliram Gaikwad , Pathan Afroz , Mohammad Naiyaz Ahmad , Grace Kaul , Manjulika Shukla , Srinivas Nanduri , Arunava Dasgupta , Sidharth Chopra , Venkata Madhavi Yaddanapudi

PII: S0022-2860(20)31860-3
DOI: https://doi.org/10.1016/j.molstruc.2020.129545
Reference: MOLSTR 129545

To appear in: *Journal of Molecular Structure*

Received date: 30 September 2020
Revised date: 26 October 2020
Accepted date: 29 October 2020

Please cite this article as: Nikhil Baliram Gaikwad , Pathan Afroz , Mohammad Naiyaz Ahmad , Grace Kaul , Manjulika Shukla , Srinivas Nanduri , Arunava Dasgupta , Sidharth Chopra , Venkata Madhavi Yaddanapudi , Design, Synthesis, in vitro and in silico evaluation of new 3-phenyl-4,5-dihydroisoxazole-5-carboxamides active against drug-resistant Mycobacterium tuberculosis, *Journal of Molecular Structure* (2020), doi: https://doi.org/10.1016/j.molstruc.2020.129545

Highlights:

- 3-phenyl-4,5-dihydroisoxazole-5-carboxylic acid derivatives were synthesized by click reaction in good yields.
- All the compounds were evaluated for their anti-microbial activity
- Compound **6f**, **6h**, **6k**, and **10a** were found to be potent against drug-resistant Mtb.
- **6k** is also effective against INH and STR -resistant Mtb with MIC 4 µg/mL and 2 µg/mL respectively
- All active derivatives were found non-toxic against Vero cells and exhibited excellent SI.

Design, Synthesis, *in vitro* and *in silico* evaluation of new 3-phenyl-4,5-dihydroisoxazole-5-carboxamides active against drug-resistant *Mycobacterium tuberculosis.*

Nikhil Baliram Gaikwad [a], Pathan Afroz [a], Mohammad Naiyaz Ahmad [b,c], Grace Kaul [b,c], Manjulika Shukla[b], Srinivas Nanduri [a], Arunava Dasgupta[*b,c], Sidharth Chopra[*b,c], and Venkata Madhavi Yaddanapudi [*a]

[a] Department of Pharmaceutical Technology and Process Chemistry, National Institute of Pharmaceutical Education and Research (NIPER), Balanagar, Hyderabad 500037, Telangana, India.

[b] Division of Microbiology, CSIR-Central Drug Research Institute, Sitapur Road, Sector 10, Janakipuram Extension, Lucknow, 226031, Uttar Pradesh, India.

[c] AcSIR: Academy of Scientific and Innovative Research (AcSIR), Ghaziabad 201002, India

*Corresponding author: Department of Pharmaceutical Technology and Process Chemistry, National Institute of Pharmaceutical Education and Research (NIPER), Balanagar, Hyderabad 500037, Telangana, India.

E-mail address: yssmadhavi@gmail.com (Venkata Madhavi Yaddanapudi), skchopra007@gmail.com (Sidharth Chopra), a.dasgupta@cdri.res.in (Arunava Dasgupta)

Keywords: Anti-TB, Isoxazoline, *Mycobacterium tuberculosis*, Oximes, Antimycobacterial activity, 3-phenyl-4,5-dihydroisoxazole-5-carboxamide, *In silico* ADME studies, Lipinski's rule of five.

Abstract

A new series of 3-phenyl-4,5-dihydroisoxazole-5-carboxamides were designed, synthesized, and evaluated for their potency against Mtb H37Rv. Designed molecules were synthesized by one-pot cycloaddition reaction in good to excellent yields. Anti-Tubercular evaluation of all synthesized derivatives identified **6k** to be highly potent (MIC 1 µg/mL) against Mtb and drug-resistant strains. All potent derivatives were found to be non-toxic when tested against Vero cells. Also, *in silico* studies were employed to explore the binding patterns of designed compounds to target Mycobacterial membrane protein Large-3. All derivatives exhibited excellent binding patterns with the receptor. The excellent *in silico* Absorption, Distribution, Metabolism, and Excretion properties and druggability parameters positions these molecules as promising lead candidates for the future development of new drugs to treat drug-resistant Tuberculosis.

1. Introduction

Tuberculosis (TB) is a communicable disease caused due to *Mycobacterium tuberculosis* (Mtb) and is one of the top 10 deadly diseases worldwide. In 2018, TB tolled more lives than HIV, though HIV patients data also involves TB patients, with 10 million infections and 1.5 million deaths.[1] Many amongst those who developed TB (0.55 million patients) were found to be resistant to the Rifampicin (RIF), which is a front-line drug utilized against TB along with Isoniazid (INH). Recently, WHO announced "The End TB strategy" to eradicate TB from the world by 2035.[2, 3] One of the goals in this strategy is to develop new chemical entities with anti-TB potential as drugs in order to tackle drug-resistance which is a major hindrance to the eradication of TB. With TB acquiring resistance against the current drug regimen, there is an urgent unmet need for the development of new drugs.

In line with our efforts towards the development of new anti-TB agents, the Isoxazoline scaffold was explored based on potential anti-TB molecules reported in the literature. Cycloserine, a second-line anti-TB drug, inhibits cell wall biosynthesis in Mtb and is a cyclic derivative of D-alanine existing in isoxazolidinone-isoxazoline tautomeric structures (Fig. 1).[4, 5] Lee *et al.* reported compounds based on nitrofuranylisoxazoline scaffold with potent inhibitory activity against Mtb and the lead molecule was "Lee-878" (Fig. 1). Lee-878's activity was predominantly due to nitrofuran scaffold and Isoxazoline existed as a bioisosteric replacement for amide linkage.[6] This paved the way for more research on various isoxazole and isoxazoline derivatives as anti-TB agents. Thereafter, isoxazoline ester derivative A without a nitrofuran ring was reported by Tangallapally *et al*.[6, 7] which also exhibited good anti-TB activity. A study by Reddy *et al*.[8] suggested isoxazoline and heterocycle hybrids were found to possess good anti-microbial activity. Mandawad *et al*. in 2014 reported novel thiophene substituted isoxazoline derivative D as Anti-TB agent.[9] In 2006, Viswajanani *et al* from Ranbaxy Ltd. reported isoxazoline amide B (Fig. 1) derived from L-phenyl alanine indicated as cell adhesion inhibitor acting as an anti-inflammatory agent [10] and indicated for bronchial asthma. A further search of reported literature directed us to BM212 [11] a pyrrole derivative that is active against Mtb and acts as a MmpL3 inhibitor. Based on this compound, many pyrrole and pyrazole based MmpL3 inhibitors were designed previously by many research groups using high-throughput screening (HTS) and scaffold hopping methods.[12, 13] One of the hits was Rimonabant, an anti-obesity drug, and its analogues have been repurposed for Mtb owing to its similarity to BM212.[14, 15] The lipophilic nature of Rimonabant enabled it to cross the blood-brain barrier. This property was primarily

suggested to be effective in cerebral TB, later the drug was withdrawn from the market due to the adverse side effects (e.g. depressive disorder). Thus, there is opportunity for researchers to reduce the side effects of the Rimonabant without losing its anti-TB potential. So, Rimonabant was found to be a promising lead for further development. Based on the reported literature on the Isoxazoline scaffold, a shape-based strategy was adapted incorporating important structural features of BM212, Rimonabant, and isoxazoline scaffold that led us to 3-phenyl-4,5-dihydroisoxazole-5-carboxamide derivatives. The designed molecules were found to have good structural alignment with BM212 as well as Rimonabant (Fig. 2) making it pharmacophorically more similar in terms of binding interactions with receptor protein, primarily indicating that designed molecules are plausible MmpL3 inhibitors. This was substantiated through our *in silico* studies. 3,5-aryl-substituted isoxazolines, as well as 5-phenyl-4,5-dihydroisoxazole-3-carboxylic acid derivatives, were reported but, to date not many efforts were put towards the development of anti-tubercular agents based on the 3-phenyl-4,5-dihydroisoxazoline-5-carboxamide scaffold, this inspired us to work on this scaffold. Also, interestingly the Kozikowski group has worked extensively on the indole-2-carboxamide (Fig. 1) derivatives with alicyclic amines as a MmpL3 inhibitors. The reported amides with the aliphatic amines were found to be ~4-300 times more potent than the aromatic amide derivatives. Subsequently, the SAR studies suggested that a) lipophilic and bulky substituents at amide nitrogen were vital for the potent anti-TB activity. b) the polar group on amidic nitrogen led to loss of activity. Also the designed molecules were potently active on the MDR and XDR TB strains.[16-18] Based on the aforementioned literature the isoxazoline caboxamide series with diverse aliphatic amines were designed and synthesized. The preliminary structure-activity relationships (SAR) of 3-phenyl-4,5-dihydroisoxazole-5-carboxamide derivatives as anti-TB agents and *in silico* assessment based on studies involving molecular docking, Absorption, Distribution, Metabolism, and Excretion studies, and druggability based on compliance to Lipinski's rule of five have been presented in the present work.

Figure 1: Previous reports on isoxazoline scaffold and amide conjugate with anti-TB activity.

Figure 2: Superimposition of Isoxazoline hybrid derivative 6k with BM212 and Rimonabant.

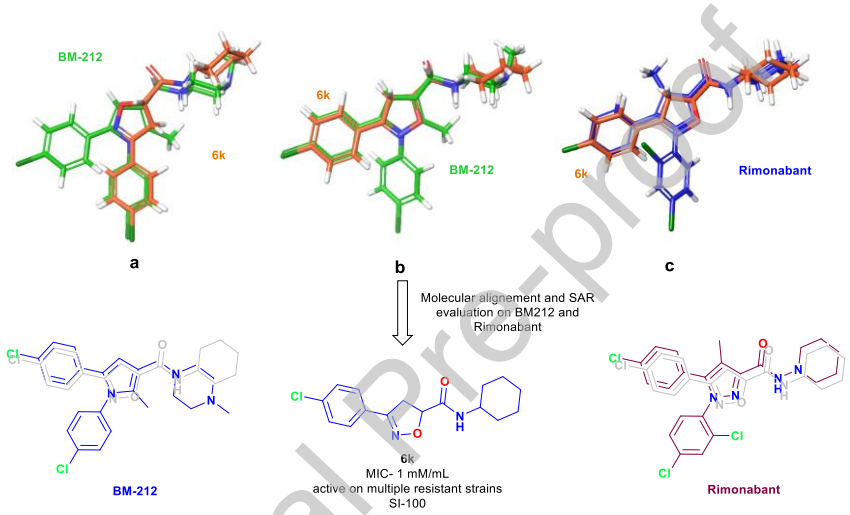

2. Results and discussion

2.1. Chemistry

All newly designed Isoxazoline derivatives were synthesized as outlined in Scheme 1. The synthesis of final derivatives involved a sequential one-pot click reaction. The first intermediate aldoxime was synthesized from commercially available substituted benzaldehydes and hydroxylamine sulphate with sodium hydroxide solution in water using a reported procedure [19, 20] with slight modifications which generated corresponding aldoximes **2** in good yield and purity. Thus, obtained aldoximes were further converted to key intermediate substituted hydroxybenzimidoyl chloride by chlorination using NCS in acetonitrile to get (E/Z)-N-hydroxybenzimidoyl chloride **3**.[21] At last, the key intermediate substituted(E/Z)-N-hydroxybenzimidoyl chlorides **3** were coupled with different

acrylamides using click reaction. The procedure followed a sequential addition of the acrolyl chloride to the amine and triethylamine solution in DCM leading to form acrylamide as intermediate to which the substituted (E/Z)-N-hydroxybenzimidoyl chloride **3** along with one equivalent of triethylamine was added which finally generated the isoxazoline derivatives (**6a-6k, 7a-7e, 8a-8e, 9a-9d, 10a-10e, 11a-11e,** and **12a-12d**) in good yield and purity.[22, 23] The one pot procedure was followed for synthesizing the entire series of molecules. All the newly synthesized compounds were characterized by ^{1}H NMR, ^{13}C NMR and HRMS (ESI) spectroscopic techniques.

Scheme 1: Synthetic route to isoxazoline amide compounds.

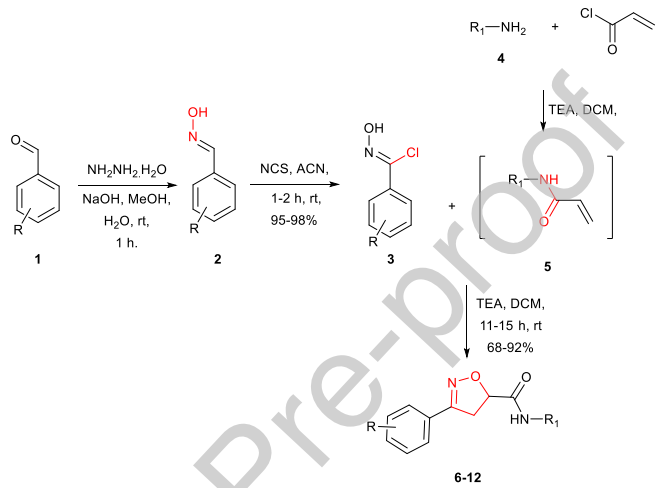

6a : R_1- Cyclohexyl, R- 2-NO_2,	7a :R1- Octyl, R- 3-Cl,	9a :R_1- Pentyl, R- 3-NO_2,	11a :R_1- Cyclopropyl, R- 3-NO_2,
6b : R_1- Cyclohexyl, R- 3-Cl,	7b :R1- Octyl, R- 4-Br,	9b :R_1- Pentyl, R- 4-F,	11b :R_1- Cyclopropyl, R- 4-F,
6c : R_1- Cyclohexyl, R- 4-Me,	7c :R1- Octyl, R- 3-F,	9c :R_1- Pentyl, R- 4-Cl,	11c :R_1- Cyclopropyl, R- 4-Br,
6d : R_1- Cyclohexyl, R- 4-CN,	7d :R1- Octyl, R- Ph,	9d :R_1- Pentyl, R- 2-NO_2,	11d :R_1- Cyclopropyl, R- 4-Cl,
6e : R_1- Cyclohexyl, R- 4-Br,	7e :R1- Octyl, R- 4-F.		11e :R_1- Cyclopropyl, R- 4(4-Benzyloxy)phenyl.
6f : R_1- Cyclohexyl, R- 4-F,			
6g : R_1- Cyclohexyl, R- 3-F,			
6h : R_1- Cyclohexyl, R- 4-NO_2,	8a :R1- Cycloheptyl, R- 3-F,	10a :R_1- Butyl, R- 4-F,	12a :R_1- 6-OMe-2-Aminobenzothiazole, R- Ph,
6i : R_1- Cyclohexyl, R- Ph,	8b :R1- Cycloheptyl, R- 4-F,	10b :R_1- Butyl, R- 3-F,	12b :R_1- 6-OMe-2-Aminobenzothiazole, R- 3-F
6j : R_1- Cyclohexyl, R- 3-NO_2,	8c :R1- Cycloheptyl, R- 4-Me,	10c :R_1- Butyl, R- 3-NO_2,	12c :R_1- 6-OMe-2-Aminobenzothiazole, R- 3-Cl,
6k : R_1- Cyclohexyl, R- 4-Cl,	8d :R1- Cycloheptyl, R- 4-CN,	10d :R_1- Butyl, R- 4-Br,	12d :R_1- 6-OMe-2-Aminobenzothiazole, R- 4-F,
6l : R_1- Cyclohexyl, R- 4-OH.	8e :R1- Cycloheptyl, R- 4-OMe.	10e :R_1- Butyl, R- 3-Cl.	

The analytical data was found in accordance with the reported structures. As a representative compound, the characterization of one of the potent derivative **6k** is discussed here. The ^{1}H NMR has shown characteristic doublet of doublet peak of the proton present on tertiary carbon possessing carboxyl group and broad singlet for the amidic proton at 5.12 ppm and 6.65 ppm respectively which ensured the formation of amide –NH- bond. Methylene Proton of isoxazole C-4 –CH_2- appeared as a doublet of a doublet at 3.65 ppm and also protons of the cyclohexyl group were observed as multiplets at 1.18-1.21 ppm (2H), 1.32-1.38 ppm (2H), 1.59-1.60 ppm (2H), 1.68-1.75 ppm (2H), 1.82-1.85 (1H), 1.93-1.95ppm (1H) belonging to –CH_2- and the proton of the –CH- group of cyclohexyl ring was observed as a multiplet at 3.74 ppm. Remaining all Protons on phenyl ring attached to isoxazole at C-3 appeared as doublets at 7.40 ppm and 7.60 ppm. Likewise, ^{13}C NMR interpretation of compound **6k** designates the existence of carbonyl carbon of the amide group at

169.5 ppm. The methylene (–CH_2-) carbon of the cyclohexyl ring at the para position to amine was observed at 25.4 ppm, the meta position methylene carbon at 24.7 ppm, and the ortho position methylene carbons were observed at 32.9ppm. The -CH- at the *ipso* position of the cyclohexyl was present at 48.2ppm. Coming to the isoxazoline ring carbons, the C-3, C-4, and C-5 appeared correspondingly at 156.2 ppm, 39.4 ppm, and 79.1 ppm. Lastly, the phenyl ring carbons of the *ipso*, *ortho*, *meta,* and para position of the phenyl ring appeared at 126.9 ppm, 128.2 ppm, 129.2 ppm, and 136.84 ppm respectively. All the other isoxazoline derivatives were characterized similarly by ^{1}H, ^{13}C NMR, and HRMS and were found in accordance with the depicted structures as presented in the experimental section. The HRMS (ESI) data of each compound represented as an $[M+H]^+$ or $[M+Na]^+$ peaks were found in compliance with their precise molecular formula.

2.2. *In vitro* anti-tubercular activity

All molecules (**6a-6k, 7a-7e, 8a-8e, 9a-9e, 10a-10e, 11a-11e,** and **12a-12e**) were screened for their inhibitory potential against Mtb H37Rv using Microplate Alamar Blue Assay (MABA) assay with INH and RIF as positive controls. The MIC values of these derivatives along with their CLogP values are reported in Table 1. To begin with, the cyclohexylamine based amide derivatives **6a-6k** (cyclohexyl as R_1 group) were synthesized and screened for their antitubercular potential on *M. tuberculosis* H37Rv varying substituents on phenyl ring and their positions. Significantly, all synthesized compounds **6a-6k** showed anti-TB activity (MIC 1-64 µg/mL). Compound **6k** with 4-chloro as R substitution exhibited the most potent activity in this series with (MIC 1 µg/mL, CLogP 4.376). Other halogenated derivatives also showed promising activity i.e. **6b** (3-Cl)-MIC: 16 µg/mL, **6e** (4-Br)-MIC: 16 µg/mL, **6f** (4-F)-MIC: 4 µg/mL. Also, **6h** with 4-nitro as R showed good activity with MIC of 4 µg/mL, CLogP of 4.61. From the results it was clear that the *para* substitution was favored for potent antitubercular activity, as the derivatives with *meta* or *ortho* substitutions were found to be less potent, *i.e* **6a** (2-Nitro: MIC 64 µg/mL), **6j** (3-Nitro: MIC 64 µg/mL), and **6h** (4-Nitro: MIC 4µg/mL), thus this shift in nitro group position from *para* to *meta* or *ortho* lead to 16 folds decrease in the activity. Similarly, the **6k** (4-Cl: MIC 1 µg/mL) and **6b** (3-Cl: MIC 16 µg/mL) derivatives suggested that a shift in chloro group position from para to meta lead to the 64 folds decline in potency.

With these results, the effect of ring size on activity was explored taking the 4-Fluoro phenyl group as constant. **8a-8e** with cycloheptyl group as R_1 substituent and **11a-11e** with cyclopropyl group as R_1 substituent were synthesized and compared with **6a-6n** (cyclohexyl as R_1 substituent). The results clearly illustrated the preference for cyclohexyl over cycloheptyl and cyclopropyl ring as R_1 substituent as there was no improvement in activity observed in cycloheptyl and cyclopropyl ring, although activity was retained by these modifications. In cyclopropyl series, the 4-benzyloxybenzyl

group as R was introduced which was the only compound to be moderately active in this series. Further, to know the effect of acyclic groups, open-chain aliphatic amines were also explored like octyl amine (**7a-7e**), pentylamine (**9a-9e**), and butylamine (**10a-10e**). Among all octyl amine derivatives in the **7a-7e** subseries, compound **7d** was only moderately active, and the remaining others were found to be weakly active which can be attributed to the higher hydrophobicity as well as a linear chain of octyl amine. Pentylamine and octylamine series showed similar results, but the butylamine series showed better results than the other two due to reduced hydrophobicity, which can be attributed to reduced chain size. This was exemplified by **10a**, a butylamine derivative that was the only derivative in the category of open chain aliphatic amines to have excellent anti-TB potential with MIC 8 µg/mL and CLogP 3.362. (Fig. 3) Apart from cyclic and acyclic aliphatic amines, few derivatives with heterocyclic amines (6-methoxy-2-aminbenzothiazole) were synthesized but these amide derivatives did not show any prominent anti-TB activity, in contrast, a moderate antimicrobial activity (MIC 16 µg/mL) was observed on *S. aureus*. Also, all derivatives were tested on non-tuberculous mycobacteria (NTM) and were found to be inactive. Other substituents such as 4-Me (**6c**) and 4- Cyano (**6d**) also showed good activity compared to unsubstituted derivative 6i. Thus, a total of 40 isoxazoline carboxamide derivatives with varying R and R_1 groups were synthesized. The synthesized compounds were tested for their anti-TB potential. Based on the results, it was observed that an increase in the hydrophobicity led to the loss of activity or reduction in potency, but, apart from hydrophobicity, the nature of the aliphatic group and position of substituent on phenyl ring also influenced activity.

Table1: *In vitro* evaluation of anti-TB and anti-microbial activity.

Entry	R	R1	MIC (µg/mL)					
			Mtb H37Rv ATCC 27294	*S. aureus* ATCC 29213	Mtb INH-res ATCC 35822	Mtb ETB-res ATCC 35837	Mtb STR-res ATCC 35820	Mtb RIF-res ATCC 35838
6a	2-NO2	Cyclohexyl	64	>64	NT	NT	NT	NT
6b	3-Cl	Cyclohexyl	16	>64	NT	NT	NT	NT
6c	4-Me	Cyclohexyl	16	>64	NT	NT	NT	NT
6d	4-CN	Cyclohexyl	16	>64	NT	NT	NT	NT
6e	4-Br	Cyclohexyl	16	>64	NT	NT	NT	NT
6f	4-F	Cyclohexyl	4	>64	**32**	**>64**	**32**	**>64**
6g	3-F	Cyclohexyl	64	>64	NT	NT	NT	NT
6h	4-NO2	Cyclohexyl	4	>64	**32**	**64**	**32**	**64**
6i	Ph	Cyclohexyl	32	>64	NT	NT	NT	NT
6j	3-NO2	Cyclohexyl	64	>64	NT	NT	NT	NT
6k	4-Cl	Cyclohexyl	1	>64	**4**	**>64**	**2**	**>64**
6l	4-OH	Cyclohexyl	16	>64	NT	NT	NT	NT
7a	3-Cl	Octyl	32	>64	NT	NT	NT	NT
7b	4-Br	Octyl	>64	>64	NT	NT	NT	NT
7c	3-F	Octyl	>64	>64	NT	NT	NT	NT
7d	Ph	Octyl	16	>64	NT	NT	NT	NT

7e	4-F	Octyl	>64	>64	NT	NT	NT	NT
8a	3-F	Heptyl	16	>64	NT	NT	NT	NT
8b	4-F	Heptyl	32	>64	NT	NT	NT	NT
8c	4-Me	Heptyl	32	>64	NT	NT	NT	NT
8d	4-CN	Heptyl	16	>64	NT	NT	NT	NT
8e	4-OMe	Heptyl	32	>64	NT	NT	NT	NT
9a	3-NO2	Pentyl	>64	>64	NT	NT	NT	NT
9b	4-F	Pentyl	32	>64	NT	NT	NT	NT
9c	4-Cl	Pentyl	>64	>64	NT	NT	NT	NT
9d	2-NO2	Pentyl	>64	>64	NT	NT	NT	NT
10a	4-F	Butyl	8	>64	**8**	**>64**	**1**	**>64**
10b	3-F	Butyl	32	>64	NT	NT	NT	NT
10c	3-NO2	Butyl	>64	>64	NT	NT	NT	NT
10d	4-Br	Butyl	16	>64	NT	NT	NT	NT
10e	3-Cl	Butyl	64	>64	NT	NT	NT	NT
11a	3-NO2	cyclopropyl	>64	>64	NT	NT	NT	NT
11b	4-F	cyclopropyl	32	>64	NT	NT	NT	NT
11c	4-Br	cyclopropyl	64	>64	NT	NT	NT	NT
11d	4-Cl	cyclopropyl	32	>64	NT	NT	NT	NT
11e	4-(OBn)Ph	cyclopropyl	16	>64	NT	NT	NT	NT
12a	Ph	6-OMe-2-NH2BTZ*	64	16	NT	NT	NT	NT
12b	3-F	6-OMe-2-NH2BTZ*	32	16	NT	NT	NT	NT
12c	3-Cl	6-OMe-2-NH2BTZ*	64	>64	NT	NT	NT	NT
12d	4-F	6-OMe-2-NH2BTZ*	64	>64	NT	NT	NT	NT
INH	-	-	0.03	NT	**>64**	**64**	**0.03**	**0.03**
RIF	-	-	0.03	NT	**0.03**	**0.06**	**0.03**	**>64**
LEVO	-	-	NT	0.125	**0.5**	**0.06**	**0.12**	**0.12**
ETB	-	-	**0.5**	NT	**2**	**>64**	**0.5**	**2**
STR	-	-	**1**	NT	**1**	**0.5**	**>64**	**0.25**

INH = Isoniazid, RIF = Rifampicin, LEVO = Levofloxacin, ETB = Ethambutol, STR = Streptomycin, *BTZ = Benzothiazole.

Figure 3: Correlation between MIC and CLogP values of isoxazoline series.

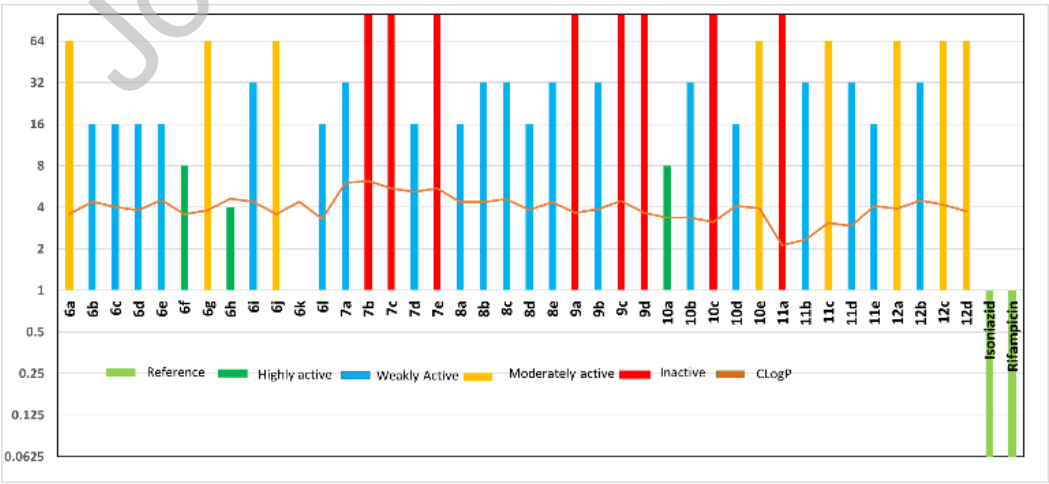

2.3. Structure-activity relationship(SAR)

The substituents present on the phenyl ring played an important role in displaying a diverse range of activity, also the position of these substitutions depicted variation in anti-TB potential. Electron withdrawing groups (NO_2, CN, Cl, and F) at para position of the acid group led to the superior anti-TB potential. Compounds with an electron-donating group at the para position were weakly active, only compound with methyl as R substituent (**6c**) was moderately active. In contrast, the electron-withdrawing group at meta positions led to the loss of anti-mycobacterial potential. Similar results were seen with the ortho position substitutions. Only para-substituted compounds were found to have good to moderate activity. It is apparent from the structure-activity relationship (SAR) analysis that cyclohexyl as R_1 substituent and Strong electron-withdrawing group at a para position such as NO_2, CN, Cl, and F as R substituents are important for the anti-mycobacterial activity. It is significant to note that the NO_2 position on the phenyl ring is crucial as **6h** (4-NO_2) is more potent than **6a** (2-NO_2) and **6j** (3-NO_2). Also, the NO_2 group acts as a hydrogen bond acceptor which plays a crucial role in binding with the receptor. Thus, similar electronic effects and interactions are seen with cyano groups and halogens acting as hydrogen bond acceptors. These groups possibly make a more promising impact on ligand binding which eventually leads to good activity. SAR interpretations are illustrated in Fig. 4.

Figure 4: SAR inferences on isoxazoline carboxamide derivatives

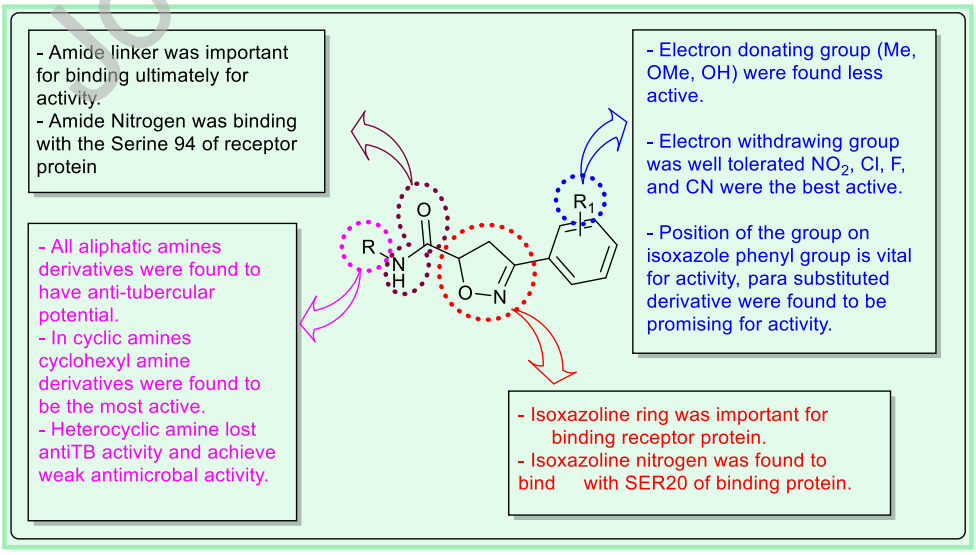

2.4. Cytotoxicity against Vero cells

Cytotoxicity assay was performed against Vero cells (ATCC CCL-81) by using MTT assay to study the influence of **6f, 6h, 6k,** and **10a** on mammalian cells. The results were depicted in CC_{50} which is the lowest concentration of compound leading to a 50% reduction in cell viability. All experiments were performed in triplicate and used Doxorubicin as a reference standard. Results revealed that compounds **6f, 6h, 6k,** and **10a** were found nontoxic to Vero cells with a CC_{50} of more than 100 µg/mL and have shown encouraging Selectivity Index (SI). The results achieved are tabulated in Table 2.

Table 2: Cytotoxicity and Selectivity index (SI) of compounds against Vero cells

2.5. Activity against drug-resistant TB strains

Entry	Mtb H37Rv MIC (µg/mL)	CC_{50} (µg/mL)	SI (CC_{50}/MIC)
6f	4.0	>100	>25
6h	4.0	>100	>25
6k	**1.0**	>100	**>100**
10a	8.0	>100	>12.5

To study the spectrum of activity of most potent derivatives (**6f, 6h, 6k,** and **10a**), these were further examined against single drug-resistant strains of Mtb which revealed that all the screened molecules

were active on INH resistant Mtb strain. Compound **6f** and **6h** showed inhibitory activity with MIC 32µg/mL, compound **6k** showed MIC of 4 µg/mL, and compound **10a** MIC 8 µg/mL. Against Ethambutol (**ETB**) and **RIF** resistant strains, only compound **6h** was found active with MIC 64 µg/mL. The compounds also showed similar activity on streptomycin (**STR**) resistant strain except for compound **10a** which exhibited potent activity with MIC of 1 µg/mL. Compound **6k** also displayed excellent activity at MIC of 2 µg/mL. These studies put forward that all tested derivatives were active on at least two resistant strains and compound **6h** found to be active on all single resistant strains which show its ability to act against drug-resistance strains. The screening results on resistant strains are presented in Table 1.

2.6. Docking study with Mycobacterial membrane protein Large 3 (MmpL3) of Mtb H37Rv.

The designing of molecules was carried out by using structural alignment and superimposition module of Schrödinger suite on BM212 and Rimonabant *i.e.* a reported MmpL3 inhibitor. The visualization of anti-TB activity inspired us to calculate binding energy studies as well as a binding pattern of designed molecules on the mycobacterial membrane protein Large (MmpL) protein. The MmpL transporters are vital for the structure as well as the pathogenesis of Mtb by ferrying trehalose monomycolates to the mycobacterial cell wall.[15] All synthesized 40 molecules were docked into the active site of protein as shown in Fig. 5. The binding energies predicted by the software were listed in Table 3. Each one of these compounds possessed distinctive substitutions at the 2^{nd}, 3^{rd}, and 4^{th} position of phenyl ring attached on isoxazoline to ensure the effectiveness of a functional group on binding interaction. Docking experiments carried out by using Schrödinger suites (2019-4) (Maestro 12.2) was carried out using Glide XP (extra precision) docking. MmpL3 protein with PDB ID: 6ajj was chosen for molecular docking studies; the protein structure was identified at 2.79 Å and has also been reported previously for docking experiments.[15, 18, 24] The docking results obtained are presented in Table 3. All the molecules exhibit good binding energy as well as XP glide scores. The isoxazole ring oxygen had hydrogen bond interaction with ALA682 of the binding site. (Fig. 6) Also, phenyl ring of isoxazole was having π-π stacking interaction with TYR646 except for compound **10a** which was having interaction with PHE649 instead of TYR646, (Fig. 5d) which suggested binding in an inverted position concerning other derivatives which allowed amidic -NH- of **10a** to make hydrogen bonding with ASH645 similar to the co-crystal ligand. The open aliphatic chain which can rotate freely makes the molecule more flexible compared to other cyclic ring compounds and makes it possible to bind in an inverted position. This could be the reason behind the anomalous activity of the **10a** derivative compared to the other aliphatic amide derivatives. Compound **6k** had excellent binding interactions with neighboring amino acids, a *p*-Cl group made halogen bond interactions with SER643, GLU647, and VAL648 while the chlorophenyl ring forms π-π stacking

interactions with TYR646.(Fig. 6c) The oxygen of the isoxazole ring had hydrogen bonding with ASH256, along with a cyclohexyl ring oriented towards the hydrophobic pocket.(Fig. 5b) These prominent interactions with binding pocket explain the higher anti-TB activity of this compound over others. All other derivatives were found to have hydrophobic interactions with LEU642, ILE253, TYR646, VAL648, PHE649, ILE679, ALA682, ILE261, PHE260, TYR257, and VAL290, and polar hydrophilic interactions with THR644, SER293, THR289, and SER286. The above molecular docking results insinuated that a plausible mechanism of anti-TB activity of the designed molecules is by inhibition of MmpL3.

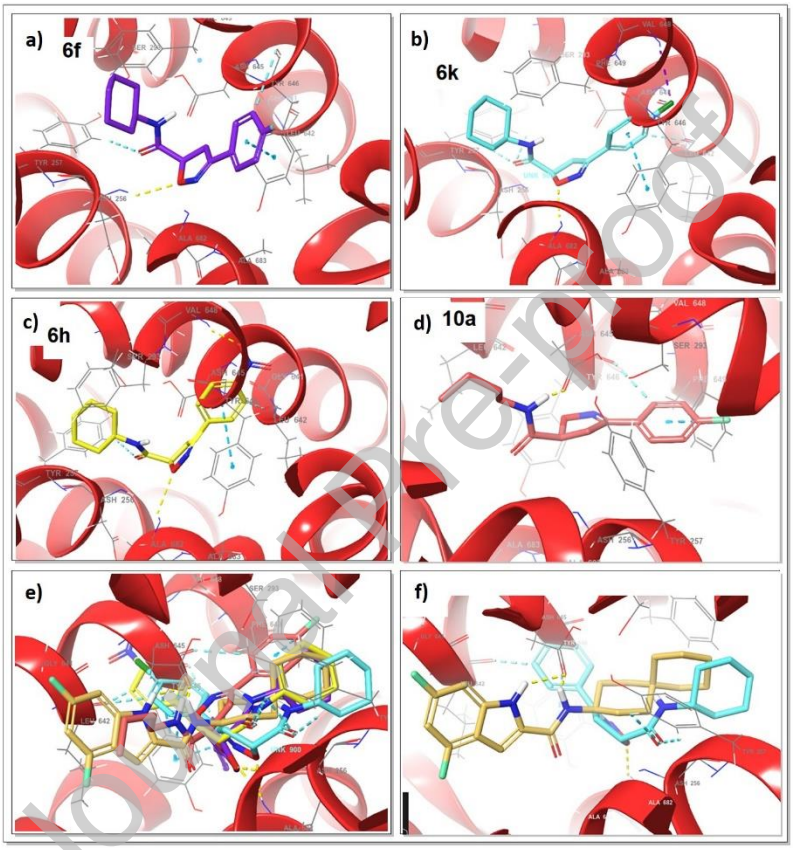

Figure 5: Ligand interactions between most active molecules and receptor protein. a) Compound **6f** (Purple) in the binding pocket of MmpL3 protein, exhibited π-π stacking interactions with TYR646. b) Compound **6k** (Sky-blue) in the binding pocket of MmpL3 protein. c) Compound **6h** (yellow) in the binding pocket of MmpL3 protein, exhibited π-π stacking interactions with TYR646. d) Compound **10a** (pink) displayed hydrogen bonding with ASH645. e) Compound **6f**, **6h**, **6k**, and **10a**, and co-crystal ligand in the binding pocket depicted a similar binding pattern of all active derivative except **10a** which bound inverted relative to others. f) Co-crystal ligand and compound **6k** superimposition show a similar binding pattern.

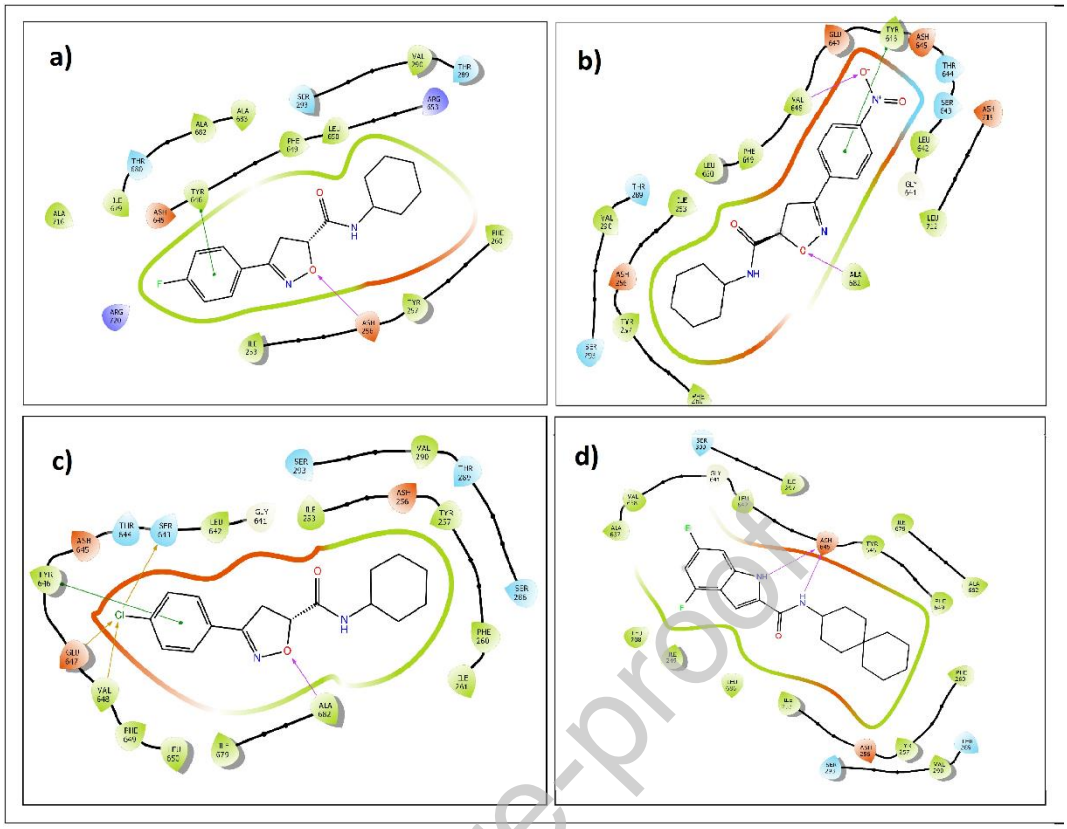

Figure 6: 2D Ligand interactions between most active molecules, co-crystal, and receptor protein (6AJJ). a) 2D Ligand interaction diagram representing compound **6f** in the binding pocket. b) Interactions diagram for the compound **6h** exhibited π-π stacking interactions with TYR646 shown by the green line. c) Representation of compound **6k** associated with multiple interactions as π-π stacking interactions with TYR646, hydrogen bonding with ALA682, and a yellow line representing the Halogen bond interactions. d) 2D representation of Co-crystal ligand observed to have hydrogen bond interactions with ASH645 denoted by the pink line.

Table 3: Anti-tubercular and *In-silico* study of the synthesized compounds on Mycobacterial membrane protein Large 3 (MmpL3-6AJJ).

Entry	MIC (µg/ ml)	XP G score (kcal/mol)	ΔG binding energy	H- bond	
				Ligand	Amino acid
6b	16	-10.239	-63.101	-C=O-NH-	TYR257
6c	16	-10.050	-59.822	-C=O-NH-	TYR257
6d	16	-10.531	-71.375	-C=O-NH-	TYR257
6e	16	-10.369	-65.854	-C=O-NH-	TYR257
6f	4	-10.266	-54.592	-C=O-NH- -O-N=(ring)	TYR257 ASH256
6h	4	-10.173	-75.823	-C=O-NH- -NO2 -O-N=(ring)	TYR257 VAL548 ALA682
6k	1	-10.413	-68.141	-C=O-NH- -O-N=(ring)	TYR257 ALA682
7a	32	-11.420	-74.777	-C=O-NH-	TYR257
7d	16	-10.402	-76.168	-C=O-NH-	TYR257
8a	16	-11.287	-70.871	-C=O-NH-	TYR257
10a	8	-9.761	-59.56	-C=O-NH-	ASH645
10d	16	-10.005	-63.283	-C=O-NH-	ASH645
11e	16	-11.129	-77.065	-C=O-NH-	ASH645
12b	32	-10.908	-82.547	-C=O-NH-	TYR257
Co-crystal ligand	-	-13.204	-88.053	-C=O-NH-	ASH645

2.7 Prediction of *in silico* absorption, distribution, metabolism, and excretion properties

ADME (absorption, distribution, metabolism, and excretion) parameters of molecules serve as stalwart points to establish their drug likeliness topographies. Thus, the ADME parameters of designed isoxazoline amides were determined by using the Qikprop module of the Schrödinger suite. Many approved drugs are found to follow the predefined set of parameters such as partition coefficient of n-octanol /water, polar surface area (PSA), aqua solubility (QPlogS), central nervous system activity (CNS), a number of likely metabolic reactions (metab), Predicted skin permeability (QPlogKp), predicted IC_{50} for the blockage of HERG K+ channels (QPloghERG), Caco-2 cell permeability (QPPCaco), human serum albumin binding (QPlogKhsa), blood/brain partition co-efficient (QPlogBB), human oral absorption, and percent human oral absorption.[25] The projected drug likeliness properties of all derivatives were found to be within the mentioned standard parameters. QPPCaco is a descriptor to predict Caco-2 cell permeability of molecule in nm/sec (>500 is great absorption, <25 is poor absorption), it is a human absorption process by the non-active transport mechanism across the gut-blood barrier.[26] The predicted QPPCaco value for isoxazoline

derivatives illustrate that designed compounds will certainly get absorbed through the gut layer. For the target molecule to become CNS active, it must have a CNS value more than or equal to 2 if its –2 (inactive) to +2 (active) scale.[26, 27] The predicted value for the CNS was in the range of -1 to -2 (table with observed values provided in supporting information). Thus, designed molecules will certainly be inactive on CNS. The Log BB values help to determine the distribution of the compound in the brain. If the compound is having log BB more than 0.3, it is predicted to cross the blood-brain barrier and if it's less than -1.0 those compounds will be weakly distributed to the brain. All molecules exhibited LogBB in a negative value, thus CNS and logBB suggest that the designed molecules will not affect CNS. Furthermore, the QPlog HERG value denotes the predicted IC_{50} value for the blockage of HERG K+ channels. Designed compounds demonstrated good predicted pharmacological properties like HERG K+ channel (HERG K+), QPlogKhsa which predicts binding to human serum albumin, QPPMDCK predicts MDCK cell permeability, MDCK cells are considered to be a good mimic for the blood-brain barrier, and QP logKp predicts the skin permeability of the molecule. Also, the percent absorption values of the majority of the compound were found to be in the range of 71-100%. None of the designed derivatives violated the rule of three as well as the rule of five. The values of predicted descriptors are presented in Table 4. The observed values suggest that all active molecules of all series exhibit a good ADME profile, which suggests that these molecules can be taken for further biological evaluation in order to develop potential anti-TB agents.

Table 4: *In-silico* ADME properties of compounds of series 6, 7, 8, 9, 10, 11, and 12.

ENTRY	CNS	QPlog S	QPlog HERG	QPP Caco	QP logBB	QPP MDCK	QP logKp	Metab	QP log Khsa	Human Oral absorption	% Human Oral absorption	Rule Of five	Rule Of three
6a	-1	-3.028	-3.37	338.65	-0.837	263.52	-3.095	3	-0.289	3	81.62	0	0
6b	0	-4.272	-3.787	1184.9	-0.119	2509.1	-2.163	2	-0.063	3	100	0	0
6c	0	-4.105	-3.794	1180.9	-0.3	1015.7	-2.194	3	-0.021	3	96.82	0	0
6d	-2	-4.331	-3.995	248.1	-1.101	185.25	-3.349	2	-0.346	3	78.47	0	0
6e	0	-4.398	-3.823	1187.2	-0.109	2701.4	-2.166	2	-0.039	3	100	0	0
6f	0	-3.913	-3.747	1180.7	-0.172	1832.2	-2.134	2	-0.133	3	96.40	0	0
6g	0	-3.898	-3.742	1177.9	-0.17	1833.5	-2.132	2	-0.134	3	96.37	0	0
6h	-2	-3.516	-3.806	141.23	-1.339	101.97	-3.904	3	-0.226	3	74.12	0	0
6i	0	-3.556	-3.865	1189.6	-0.278	1016.5	-1.997	2	-0.174	3	95.09	0	0
6j	-2	-3.506	-3.802	141.55	-1.335	102.64	-3.899	3	-0.227	3	74.14	0	0
6k	0	-4.303	-3.8	1190.3	-0.122	2501.0	-2.167	2	-0.062	3	100	0	0
6l	-1	-3.391	-3.754	362.33	-0.886	278.89	-3.059	3	-0.304	3	81.713	0	0
7a	-1	-5.281	-4.674	746.29	-0.782	1676.3	-1.893	2	0.184	3	100	0	0
7b	-1	-5.321	-4.585	874.90	-0.701	2013.9	-1.811	2	0.185	3	100	0	0
7c	-1	-4.903	-4.647	747.72	-0.83	1229.5	-1.859	2	0.109	3	100	0	0
7d	-1	-4.464	-4.668	874.46	-0.868	759.80	-1.639	2	0.046	3	100	0	0
7e	-1	-4.901	-4.552	875.37	-0.777	1334.8	-1.797	2	0.089	3	100	0	0
8a	0	-4.293	-3.777	1051.1	-0.238	1569.6	-2.245	2	-0.01	3	96.97	0	0
8b	0	-4.334	-3.822	1061.8	-0.239	1585.2	-2.239	2	-0.01	3	100	0	0
8c	0	-4.542	-3.876	1060.2	-0.372	875.3	-2.302	3	0.104	3	100	0	0
8d	-2	-4.933	-4.057	220.48	-1.175	160.2	-3.455	2	-0.224	3	79.04	0	0
8e	0	-4.175	-3.844	1058.0	-0.429	873.1	-2.208	3	-0.048	3	96.16	0	0
9a	-2	-3.503	-4.111	104.48	-1.741	74.08	-3.859	3	-0.339	3	71.79	0	0
9b	0	-3.765	-4.08	821.27	-0.566	1220.4	-2.155	2	-0.244	3	93.20	0	0
9c	0	-4.134	-4.118	819.45	-0.517	1664.9	-2.189	2	-0.172	3	94.69	0	0
9d	-2	-3.433	-4.112	151.53	-1.543	110.61	-3.49	3	-0.341	3	75.44	0	0
10a	0	-3.346	-3.878	820.74	-0.477	1219.0	-2.253	2	-0.357	3	90.99	0	0
10b	0	-3.339	-3.876	819.40	-0.477	1217.8	-2.252	2	-0.357	3	90.97	0	0
10c	-2	-3.145	-3.944	97.54	-1.67	67.59	-4.024	3	-0.447	3	68.95	0	0
10d	0	-3.831	-3.95	821.21	-0.42	1787.6	-2.289	2	-0.263	3	92.94	0	0
10e	0	-3.707	-3.917	819.61	-0.429	1662.3	-2.286	2	-0.286	3	92.45	0	0
11a	0	-2.913	-3.774	722.64	-0.366	1152.2	-2.489	2	-0.471	3	87.083	0	0
11b	0	-2.913	-3.774	722.64	-0.366	1152.1	-2.489	2	-0.471	3	87.083	0	0
11c	0	-3.391	-3.837	731.58	-0.305	1700.6	-2.52	2	-0.382	3	89.089	0	0
11d	0	-3.285	-3.822	722.88	-0.319	1571.8	-2.522	2	-0.401	3	88.583	0	0
11e	-1	-4.907	-5.545	735.73	-0.79	644.82	-1.528	4	0.06	3	100	0	0
12a	0	-4.75	-6.516	1084.3	-0.471	1004.5	-1.807	3	-0.02	3	100	0	0
12b	0	-5.319	-6.287	1081.1	-0.453	1806.4	-2.042	4	0.019	3	100	0	0

*Calculations were done by using the Qikprop module of Schrödinger Suite 2019-02

2.7. Lipinski's rule-of-five

Additionally, to evaluate the drug-likeness of these synthesized derivatives, these were checked for compliance with Lipinski's rule-of-five(RO5)/ Pfizer's rule of five *i.e*. Molecular weight (MW) ≤ 500D, partition coefficient (logP) values ≤5, Number of hydrogen bond donors ≤ 5, Number of hydrogen bond acceptors ≤10, No of rotatable bonds ≤10. [28, 29] (Details of these findings along with descriptors are depicted in Table 5). The results illustrate that all the derivatives of this series exhibit excellent pharmacokinetic properties and might be useful for the future development of novel lead molecules. Descriptor values for the most potent derivatives are described in Table 5

Table 5: Descriptors of Lipinski's rule-of-five and calculated values.

Entry	Mol_MW	HB Donor	HB Acceptor	No. of Rotatable bonds	QPlogPo/w
6a	317.344	1	6.2	3	1.605
6b	306.791	1	5.2	2	2.727
6c	286.373	1	5.2	2	2.543
6d	297.356	1	6.7	2	1.48
6e	351.242	1	5.2	2	2.805
6f	290.337	1	5.2	3	2.472
6g	290.337	1	5.2	2	2.471
6h	317.344	1	6.2	2	1.485
6i	272.346	1	5.2	2	2.238
6j	317.344	1	6.2	2	1.485
6k	306.791	1	5.2	3	2.729
6l	288.346	2	5.95	3	1.531
7a	336.861	1	5.2	8	3.817
7b	381.312	1	5.2	8	3.871
7c	320.406	1	5.2	8	3.557
7d	302.416	1	5.2	8	3.302
7e	320.406	1	5.2	8	3.531
8a	304.363	1	5.2	2	2.723
8b	304.363	1	5.2	2	2.726
8c	300.4	1	5.2	2	2.8
8d	311.383	1	6.7	3	1.733
8e	316.399	1	5.95	3	2.576
9a	305.137	1	6.2	6	1.487
9b	278.143	1	5.2	5	2.407
9c	294.113	1	5.2	5	2.664
9d	305.137	1	6.2	6	1.617
10a	264.299	1	5.2	4	2.031
10b	264.299	1	5.2	4	2.029
10c	291.306	1	6.2	5	1.094
10d	325.204	1	5.2	4	2.362
10e	280.753	1	5.2	4	2.284
11a	248.256	1	5.2	2	1.532
11b	248.256	1	5.2	2	1.532
11c	309.162	1	5.2	2	1.858
11d	264.711	1	5.2	2	1.787
11e	336.39	1	5.95	5	3.213
12a	323.369	1	6.7	2	2.786
12b	371.385	1	7.45	3	3.104
12c	387.0444	1	7.45	3	4.161
12d	371.385	1	7.45	3	3.104
Std. range	<500	0-5	5-10	0-15	-2.5-6.5

*Calculations were done by using the Qikprop module of Schrödinger Suite 2019-02

3. Conclusions

In conclusion, a series of new 3-phenyl-4,5-dihydroisoxazole-5-carboxamide derivatives (**6a-6m**), (**7a-7e**), (**8a-8e**), (**9a-9d**), (**10a-10e**), (**11a-11e**), (**12a-12d**) were designed and synthesized in very good yields and evaluated for anti-TB potential. The synthesized derivatives were characterized by NMR and HRMS. All derivatives were evaluated for their *in vitro* anti-TB activity against Mtb H37Rv. Amongst all, compound **6f** (MIC: 4 µg/mL), **6k** (MIC: 1µg/mL), **6h** (MIC: 4 µg/mL), and **10a** (MIC: 8 µg/mL) were most active derivatives. Also, these molecules were active against drug-resistant strains of Mtb. Cytotoxicity assessment on Vero cells (ATCC CCL-81) by using MTT assay demonstrated that all the derivatives tested were notably non-toxic along with excellent SI (**6k** SI-100). To substantiate the design of these molecules, activity studies, and to identify the binding pattern of these derivatives, molecular modelling studies were carried out on the MmpL3 protein,(PDB id: 6ajj), which illustrated excellent binding energy together with binding interactions with the receptor-binding pocket. Docking results demonstrated the synergy in the binding energy with the activity of reported molecules. This insinuates MmpL3 as a plausible target for these molecules. Further, these molecules were evaluated for *in silico* ADME properties. Results stated that all observed descriptor values for designed molecules were in agreement with standard values. In addition, physicochemical parameters of all derivatives were following Lipinski's rule-of-five, thus exhibiting excellent druggability. As there is an urgent unmet need for newer anti-TB agents active against drug-resistant TB, an attempt has been made to overcome the shortcomings of Rimonabant by incorporating the isoxazoline carboxamide scaffold and studying the effect of lipophilicity through ADME studies of the synthesized derivatives. These results primarily indicate that this scaffold has the potential for further optimization and improvement. Further efforts in this direction are in progress.

4. Experimental section

4.1. Materials and methods

All the required chemicals, reagents, and starting materials were procured from commercial providers and were used as such. The monitoring of reactions was performed by TLC-MERCK pre-coated silica gel 60-F254 (0.5 mm) aluminium plates under UV light. ^{1}H and ^{13}C NMR spectra were obtained on Bruker Avance 500 MHz spectrometer operating at 500 MHz for proton (^{1}H) and 125 MHz for carbon (^{13}C) spectrometry using tetramethylsilane (TMS) as the internal standard and chemical shifts are reported in ppm. Chemical shifts are in reference to TMS (δ 0.00 for ^{1}H NMR and ^{13}C NMR), DMSO-D_6 appeared at (δ 2.50 for ^{1}H NMR and 39.7 for ^{13}C NMR) or $CDCl_3$ (δ 7.26 for ^{1}H

NMR and 77.00 or 77.16 for ^{13}C NMR) or combination of $CDCl_3$ and DMSO-D_6. Spin multiplicities are reported as s (singlet), brs (broad singlet), d (doublet), dd (double doublet), t (triplet), and m (multiplet). Coupling constant (J) values are reported in hertz (Hz). HRMS were determined with Agilent QTOF mass spectrometer 6540 series instrument and were performed in the ESI techniques at 70 eV. Melting points were taken using Stuart® SMP30 apparatus.

5. Synthesis and procedures

5.1. General procedure for the preparation of compounds 2

Compound 2a-l were synthesized according to the procedures described in the literature [19, 20]To a solution of substituted aldehyde (1 mmol) in ethanol/ methanol (5 mL) the solution of $(NH_2OH)_2.SO_4$ (0.6 mmol, 0.6 eq.) and NaOH (1.2 mmol, 1.2 eq.) in water (25ml) at 0°C were added dropwise. After addition cooling was removed and the reaction mixture was continued to stir at room temperature for 1-2 h (depending on aldehyde). After the completion of reaction indicated by the TLC, the reaction mixture was evaporated under reduced pressure to remove organic solvent which leaves oily liquid at the base of aqueous layer. To which crushed ice was added and resulting solid was filtered. Crude product was crystallised of from EtOH gave the compound **2**

5.2. General procedure for the preparation of compounds 3a-3l

Compound 3a-l were synthesized based on previous synthetic procedures.[21] To a solution of substituted aldoxime (0.5 mmol, 1eq.) in acetonitrile (10 mL) the n-chlorosuccinimide (NCS)(0.55 mmol, 1.1 eq.) was added slowly at 0°C. The reaction mixture stirred for 15min at 0°C then cooling was removed and stir at room temperature for 1-2h. Completion of reaction indicated by the TLC; the reaction mixture was evaporated under reduced pressure. To the liquid residue obtained 20 mL water was added and the resulting aqueous solution was extracted with Ethyl acetate (20 mL x 3). Combined organic layer was washed with dil. Hydrochloric acid (0.1N) to remove residual succinimide, followed by brine wash. The organic layer was dried over anhydrous Na_2SO_4 and concentrated *in vacuo* to obtain a clear crystalline compound **3a**, which was directly used in the next step without further purification. Substituted chloro-aldoxime **3b-3l** were synthesized using same method.

5.3. General procedure for the preparation of compounds 6, 7, 8, 9, 10, 11, and 12 series

To a cooled (0°C) solution of amine **4** (0.2mmol, 1 eq.), triethylamine (0.21mmol, 1.05eq.) in dichloromethane (DCM) (10 mL) acrolyl chloride (0.21mmol, 1.05 eq.) was added slowly over 4-5 min and stirred for 45 min at 0°C. Reaction monitored by TLC, after completion of amine another portion

of triethylamine (0.21mmol, 1.05eq.) was added to the reaction mixture and stirred for another 10min and substituted chloroaldoximes **3a-3l** were added slowly in cooling condition. After 15 min cooling bath was removed and continued to stir at room temperature for overnight. Upon completion of the reaction DCM was evaporated *in vacuo* and 25ml water was added. The aqueous layer was extracted with ethyl acetate (20 mL x 3). The combined organic layer was dried over anhydrous Na_2SO_4 and concentrated under reduced pressure to get off white coloured crude solid product. Crude product obtained was crystallised from ethanol : ACN mixture.

5.3.1. N-cyclohexyl-3-(2-nitrophenyl)-4,5-dihydroisoxazole-5-carboxamide **(6a)**.

White solid, Yield: 68%, m.p. 101°C, ^{1}H NMR (500 MHz, $CDCl_3$) δ 8.10 (d, J = 8.1 Hz, 1H), 7.71 (t, J = 7.5 Hz, 1H), 7.67 – 7.61 (m, 1H), 7.51 (d, J = 7.6 Hz, 1H), 6.67 (s, 1H), 5.18 (dd, J = 11.2, 5.5 Hz, 1H), 3.86 – 3.79 (m, 1H), 3.63 (td, J = 17.3, 11.5 Hz, 2H), 1.96 (t, J = 12.3 Hz, 2H), 1.78 – 1.71 (m, 3H), 1.66 – 1.60 (m, 1H), 1.43 – 1.34 (m, 2H), 1.24 – 1.18 (m, 2H).; ^{13}C NMR (126 MHz, $CDCl_3$) δ 169.29, 156.37, 147.92, 133.59, 131.08, 130.72, 125.03, 124.53, 79.42, 48.28, 42.50, 32.93, 32.88, 25.43, 24.86, 24.82.; HRMS –QTOF MS/MS: m/z $[M+H]^+$ calcd for $C_{16}H_{19}N_3O_4$ 318.1454; found,318.1454.

5.3.2. 3-(3-chlorophenyl)-N-cyclohexyl-4,5-dihydroisoxazole-5-carboxamide **(6b)**.

Off White solid; Yield: 86%; m.p. 95 °C,; ^{1}H NMR (500 MHz, $CDCl_3$) δ 7.60 (d, J = 8.7 Hz, 2H), 7.40 (d, J = 8.7 Hz, 2H), 6.65 (s, 1H), 5.11 (dd, J = 10.7, 6.8 Hz, 1H), 3.79 – 3.70 (m, 1H), 3.65 (dd, J = 8.7, 4.4 Hz, 2H), 1.94 (d, J = 16.1 Hz, 1H), 1.83 (d, J = 16.3 Hz, 1H), 1.77 – 1.66 (m, 2H), 1.66 – 1.58 (m, 2H), 1.35 (tt, J = 16.3, 10.3 Hz, 2H), 1.21 – 1.14 (m, 2H).; ^{13}C NMR (126 MHz, $CDCl_3$) δ 169.55, 156.37, 136.83, 129.18, 128.25, 126.91, 79.16, 48.25, 39.47, 32.93, 32.88, 25.39, 24.78.; HRMS –QTOF MS/MS: m/z $[M+H]^+$ calcd for $C_{16}H_{20}N_2O_2Cl$: 307.1213; found, 307.1211.

5.3.3. N-cyclohexyl-3-(p-tolyl)-4,5-dihydroisoxazole-5-carboxamide (**6c**).

Off White solid; Yield: 89%; m.p. 130°C; ^{1}H NMR (500 MHz, $CDCl_3$) δ 7.56 (d, J = 8.1 Hz, 2H), 7.22 (d, J = 8.0 Hz, 2H), 6.69 (s, 1H), 5.09 (dd, J = 9.6, 7.9 Hz, 1H), 3.78 – 3.71 (m, 1H), 3.69 – 3.63 (m, 2H), 2.39 (s, 3H), 1.94 (d, J = 15.1 Hz, 1H), 1.82 (d, J = 15.5 Hz, 1H), 1.75 – 1.66 (m, 2H), 1.39 – 1.30 (m, 2H), 1.25 (s, 1H), 1.22 – 1.12 (m, 3H).; ^{13}C NMR (126 MHz, $CDCl_3$) δ 169.90, 157.18, 141.13, 129.56, 126.98, 125.60, 78.86, 48.17, 39.87, 32.94, 32.88, 25.41, 24.75, 21.46.; HRMS –QTOF MS/MS: m/z [M+H]+ calcd for $C_{17}H_{23}N_2O_2$: 287.1760; found, 287.1760.

5.3.4. 3-(4-cyanophenyl)-N-cyclohexyl-4,5-dihydroisoxazole-5-carboxamide (**6d**).

White solid; Yield: 92%; m.p. 96°C; ^{1}H NMR (500 MHz, $CDCl_3$) δ 7.75 (dd, J = 31.1, 7.5 Hz, 4H), 6.62 (s, 1H), 5.17 (dd, J = 11.3, 6.1 Hz, 1H), 3.74 (dd, J = 13.1, 7.3 Hz, 1H), 3.67 (dd, J = 19.4, 6.1 Hz, 2H), 1.95

(d, J = 11.7 Hz, 1H), 1.83 (d, J = 12.0 Hz, 1H), 1.76 – 1.67 (m, 2H), 1.62 (d, J = 12.5 Hz, 1H), 1.35 (dd, J = 15.5, 13.0 Hz, 2H), 1.23 – 1.13 (m, 3H).; ^{13}C NMR (126 MHz, $CDCl_3$) δ 169.12, 156.04, 132.69, 132.61, 127.49, 118.10, 114.13, 79.62, 48.34, 38.89, 32.90, 32.85, 25.37, 24.75.; HRMS –QTOF MS/MS: m/z $[M+H]^+$ calcd for $C_{17}H_{20}N_3O_2$: 298.1556; found, 298.1554.

5.3.5. 3-(4-bromophenyl)-N-cyclohexyl-4,5-dihydroisoxazole-5-carboxamide (**6e**).

White solid; Yield: 85%; m.p. 103°C; ^{1}H NMR (500 MHz, $CDCl_3$) δ 7.55 (q, J = 8.8 Hz, 4H), 6.64 (s, 1H), 5.12 (dd, J = 10.6, 6.9 Hz, 1H), 3.79 – 3.70 (m, 1H), 3.65 (dd, J = 8.7, 3.8 Hz, 2H), 1.94 (d, J = 14.4 Hz, 1H), 1.83 (d, J = 16.0 Hz, 1H), 1.75 – 1.66 (m, 2H), 1.40 – 1.30 (m, 2H), 1.24 (d, J = 8.8 Hz, 1H), 1.22 – 1.12 (m, 3H).; ^{13}C NMR (126 MHz, $CDCl_3$) δ 169.51, 156.47, 150.54, 132.14, 128.44, 127.36, 125.17, 79.18, 76.77, 48.25, 39.39, 32.93, 32.88, 25.39, 24.78.; HRMS –QTOF MS/MS: m/z $[M+H]^+$ calcd for $C_{16}H_{19}N_2O_2Br$: 353.0692; found, 353.0692.

5.3.6. N-cyclohexyl-3-(4-fluorophenyl)-4,5-dihydroisoxazole-5-carboxamide (**6f**).

White solid; Yield: 92%; m.p. 98°C; ^{1}H NMR (500 MHz, $CDCl_3$) δ 7.73 – 7.62 (m, 2H), 7.12 (t, J = 8.7 Hz, 2H), 6.67 (s, 1H), 5.11 (dd, J = 10.6, 6.9 Hz, 1H), 3.78 – 3.71 (m, 1H), 3.69 – 3.60 (m, 2H), 1.94 (d, J = 14.2 Hz, 1H), 1.83 (d, J = 12.6 Hz, 1H), 1.74 – 1.60 (m, 4H), 1.39 – 1.29 (m, 2H), 1.19 (dd, J = 20.7, 8.1 Hz, 2H).; ^{13}C NMR (126 MHz, $CDCl_3$) δ 169.64, 165.14, 163.14, 156.29, 129.10, 129.03, 124.71, 116.17, 116.00, 79.06, 48.23, 39.70, 32.94, 32.89, 25.40, 24.78.; HRMS –QTOF MS/MS: m/z $[M+H]^+$ calcd for $C_{16}H_{19}N_2O_2F$: 291.1509; found, 291.1509.

5.3.7. N-cyclohexyl-3-(3-fluorophenyl)-4,5-dihydroisoxazole-5-carboxamide (**6g**).

White solid; Yield: 78%; m.p. 80°C; ^{1}H NMR (500 MHz, $CDCl_3$) δ 7.41 (dd, J = 7.5, 3.8 Hz, 3H), 7.15 (dd, J = 9.7, 8.0 Hz, 1H), 6.65 (s, 1H), 5.13 (dd, J = 10.3, 7.2 Hz, 1H), 3.79 – 3.71 (m, 1H), 3.66 (dd, J = 8.8, 2.5 Hz, 2H), 1.94 (d, J = 16.2 Hz, 1H), 1.83 (d, J = 16.1 Hz, 1H), 1.72 (ddd, J = 17.9, 12.3, 6.7 Hz, 3H), 1.64 – 1.58 (m, 1H), 1.39 – 1.31 (m, 2H), 1.18 (ddd, J = 12.7, 10.4, 3.6 Hz, 2H).; ^{13}C NMR (126 MHz, $CDCl_3$) δ 169.43, 163.72, 161.75, 156.41, 130.53, 122.84, 117.81, 113.87, 79.18, 48.21, 39.41, 32.89, 32.84, 25.36, 24.75.; HRMS –QTOF MS/MS: m/z $[M+H]^+$ calcd for $C_{16}H_{19}N_2O_2F$: 291.1509; found, 291.1507.

5.3.8. N-cyclohexyl-3-(4-nitrophenyl)-4,5-dihydroisoxazole-5-carboxamide (**6h**).

White solid; Yield: 84%; m.p. 110°C; ^{1}H NMR (500 MHz, $CDCl_3$) δ 7.41 (dd, J = 7.5, 3.8 Hz, 3H), 7.15 (dd, J = 9.7, 8.0 Hz, 1H), 6.65 (s, 1H), 5.13 (dd, J = 10.3, 7.2 Hz, 1H), 3.79 – 3.71 (m, 1H), 3.66 (dd, J = 8.8, 2.5 Hz, 2H), 1.94 (d, J = 16.2 Hz, 1H), 1.83 (d, J = 16.1 Hz, 1H), 1.72 (ddd, J = 17.9, 12.3, 6.7 Hz, 3H), 1.64 – 1.58 (m, 1H), 1.39 – 1.31 (m, 2H), 1.18 (ddd, J = 12.7, 10.4, 3.6 Hz, 2H).; ^{13}C NMR (126

MHz, $CDCl_3$) δ 169.43, 163.72, 161.75, 156.41, 130.53, 122.84, 117.81, 113.87, 79.18, 48.21, 39.41, 32.89, 32.84, 25.36, 24.75.; HRMS –QTOF MS/MS: m/z $[M+H]^+$ calcd for $C_{16}H_{19}N_3O_4$: 318.1454; found, 318.1454.

5.3.9. N-cyclohexyl-3-phenyl-4,5-dihydroisoxazole-5-carboxamide **(6i).**

White solid; Yield: 76%; m.p. 102°C; ^1H NMR (500 MHz, $CDCl_3$) δ 7.67 (d, J = 6.3 Hz, 2H), 7.47 – 7.40 (m, 3H), 6.68 (s, 1H), 5.11 (dd, J = 10.1, 7.3 Hz, 1H), 3.79 – 3.71 (m, 1H), 3.70 – 3.65 (m, 2H), 1.94 (d, J = 16.1 Hz, 1H), 1.83 (d, J = 16.3 Hz, 1H), 1.72 (ddd, J = 15.2, 8.8, 2.7 Hz, 2H), 1.63 – 1.58 (m, 1H), 1.41 – 1.29 (m, 2H), 1.17 (ddd, J = 15.9, 13.5, 3.6 Hz, 3H).; ^{13}C NMR (126 MHz, $CDCl_3$) δ 157.25, 130.78, 128.90, 128.41, 127.07, 79.07, 77.30, 77.04, 76.79, 48.24, 39.90, 32.99, 32.94, 25.41, 24.81.; HRMS – QTOF MS/MS: m/z $[M+H]^+$ calcd for $C_{16}H_{19}N_2O_2$:273.1603; found, 273.1605.

5.3.10. N-cyclohexyl-3-(3-nitrophenyl)-4,5-dihydroisoxazole-5-carboxamide **(6j).**

White solid; Yield: 73%; m.p. 83°C; ^1H NMR (500 MHz, $CDCl_3$) δ 8.52 (t, J = 1.9 Hz, 1H), 8.30 (d, J = 10.3 Hz, 1H), 8.01 (d, J = 7.8 Hz, 1H), 7.63 (t, J = 8.0 Hz, 1H), 6.63 (s, 1H), 5.19 (dd, J = 11.6, 5.9 Hz, 1H), 3.77 (t, J = 6.5 Hz, 1H), 3.75 – 3.64 (m, 2H), 1.96 (d, J = 10.7 Hz, 1H), 1.84 (d, J = 14.0 Hz, 1H), 1.74 – 1.62 (m, 4H), 1.40 – 1.31 (m, 2H), 1.23 – 1.16 (m, 2H).; ^{13}C NMR (126 MHz, $CDCl_3$) δ 169.11, 155.71, 148.54, 132.47, 130.29, 130.01, 125.12, 121.89, 79.59, 48.34, 39.09, 32.91, 32.87, 25.38, 24.76.; HRMS –QTOF MS/MS: m/z $[M+H]^+$ calcd for $C_{16}H_{19}N_3O_4$: 318.1454; found, 318.1454.

5.3.11. 3-(4-chlorophenyl)-N-cyclohexyl-4,5-dihydroisoxazole-5-carboxamide **(6k).**

White solid; Yield: 90%; m.p. 83°C; ^1H NMR (500 MHz, $CDCl_3$) δ 7.60 (d, J = 8.7 Hz, 2H), 7.40 (d, J = 8.7 Hz, 2H), 6.65 (s, 1H), 5.12 (dd, J = 10.6, 6.8 Hz, 1H), 3.78 – 3.71 (m, 1H), 3.65 (dd, J = 8.7, 4.1 Hz, 2H), 1.97 – 1.91 (m, 1H), 1.86 – 1.80 (m, 1H), 1.76 – 1.67 (m, 2H), 1.59 (d, J = 3.8 Hz, 2H), 1.40 – 1.30 (m, 2H), 1.21 – 1.14 (m, 2H).; ^{13}C NMR (126 MHz, $CDCl_3$) δ 169.12, 156.04, 132.61, 127.49, 118.10, 114.13, 79.62, 48.34, 38.89, 32.90, 32.85, 25.37, 24.75.; HRMS –QTOF MS/MS: m/z $[M+H]^+$ calcd for $C_{16}H_{20}N_2O_2Cl$: 307.1213; found, 307.1213.

5.3.12. N-cyclohexyl-3-(4-hydroxyphenyl)-4,5-dihydroisoxazole-5-carboxamide **(6l).**

White solid; Yield: 70%; m.p. 123°C; ^1H NMR (500 MHz, DMSO-D_6) δ 9.96 (s, 1H), 7.99 (d, J = 8.1 Hz, 1H), 7.52 (d, J = 8.7 Hz, 2H), 6.83 (d, J = 8.7 Hz, 2H), 4.97 (dd, J = 11.3, 7.2 Hz, 1H), 3.61 – 3.55 (m, 2H), 3.50 – 3.44 (m, 1H), 1.70 (d, J = 16.5 Hz, 5H), 1.25 (dd, J = 16.2, 9.9 Hz, 5H).; ^{13}C NMR (126 MHz, $CDCl_3$) δ 170.00, 159.79, 156.89, 128.60, 126.71, 115.93, 78.52, 48.08, 39.94, 32.82, 32.77, 25.32, 24.73, 24.71.; HRMS –QTOF MS/MS: m/z $[M+H]^+$ calcd for $C_{16}H_{19}N_2O_3$: 289.1552; found, 289.1552.

5.3.13. 3-(3-chlorophenyl)-N-octyl-4,5-dihydroisoxazole-5-carboxamide (**7a**).

White solid; Yield: 78%; m.p. 56°C; ^{1}H NMR (500 MHz, $CDCl_3$) δ 7.68 (t, J = 1.8 Hz, 1H), 7.53 (d, J = 9.0 Hz, 1H), 7.42 (d, J = 8.9 Hz, 1H), 7.36 (t, J = 7.9 Hz, 1H), 6.78 (s, 1H), 5.15 (dd, J = 10.9, 6.3 Hz, 1H), 3.66 (dd, J = 8.6, 6.0 Hz, 2H), 3.31 (dt, J = 13.5, 6.7 Hz, 1H), 3.22 (dt, J = 13.3, 6.5 Hz, 1H), 1.54 – 1.48 (m, 2H), 1.29 – 1.22 (m, 10H), 0.86 (t, J = 7.0 Hz, 3H).; ^{13}C NMR (126 MHz, $CDCl_3$) δ 170.40, 156.37, 134.96, 130.75, 130.14, 130.11, 127.00, 125.12, 79.19, 39.40, 39.31, 31.74, 29.35, 29.17, 29.15, 26.81, 22.62, 14.07.; HRMS –QTOF MS/MS: m/z $[M+H]^+$ calcd for $C_{18}H_{26}N_2O_2Cl$: 337.1683; found, 337.1683. m/z $[M+Na]^+$ calcd for $C_{18}H_{26}N_2O_2ClNa$: 359.1502; found, 359.1502.

5.3.14. 3-(4-bromophenyl)-N-octyl-4,5-dihydroisoxazole-5-carboxamide (**7b**).

White solid; Yield: 72%; m.p. 106°C; ^{1}H NMR (500 MHz, $CDCl_3$) δ 7.60 – 7.49 (m, 4H), 6.78 (s, 1H), 5.14 (dd, J = 10.7, 6.4 Hz, 1H), 3.66 (dd, J = 8.6, 5.2 Hz, 2H), 3.32 (td, J = 13.5, 7.0 Hz, 1H), 3.20 (td, J = 13.1, 7.2 Hz, 1H), 1.54 – 1.48 (m, 2H), 1.29 – 1.22 (m, 10H), 0.86 (t, J = 7.0 Hz, 3H).; ^{13}C NMR (126 MHz, $CDCl_3$) δ 170.48, 156.56, 132.15, 128.44, 127.30, 125.21, 79.16, 39.44, 39.34, 31.74, 29.35, 29.17, 29.15, 26.81, 22.62, 14.07.; HRMS –QTOF MS/MS: m/z $[M+H]^+$ calcd for $C_{18}H_{26}N_2O_2Br$: 381.1178; found, 381.1178.

5.3.15. 3-(3-fluorophenyl)-N-octyl-4,5-dihydroisoxazole-5-carboxamide (**7c**).

White solid; Yield: 84%; m.p. 74°C; ^{1}H NMR (500 MHz, $CDCl_3$) δ 7.41 (ddd, J = 9.2, 4.7, 3.2 Hz, 3H), 7.19 – 7.11 (m, 1H), 6.78 (s, 1H), 5.15 (dd, J = 10.5, 6.7 Hz, 1H), 3.71 – 3.62 (m, 2H), 3.32 (td, J = 13.5, 7.0 Hz, 1H), 3.24 – 3.17 (m, 1H), 1.54 – 1.48 (m, 2H), 1.29 – 1.23 (m, 10H), 0.86 (t, J = 7.0 Hz, 3H).; ^{13}C NMR (126 MHz, $CDCl_3$) δ 170.42, 163.75, 161.78, 156.53, 130.57, 122.88, 117.87, 113.90, 79.20, 39.49, 39.34, 31.74, 29.35, 29.17, 29.15, 26.81, 22.61, 14.06.; HRMS –QTOF MS/MS: m/z $[M+H]^+$ calcd for $C_{18}H_{26}N_2O_2F$: 321.1978; found, 321.1978. m/z $[M+Na]^+$ calcd for $C_{18}H_{26}N_2O_2F.Na$: 343.1798; found, 343.1798.

5.3.16. N-octyl-3-phenyl-4,5-dihydroisoxazole-5-carboxamide (**7d**).

White solid; Yield: 88%; m.p. 103°C; ^{1}H NMR (500 MHz, $CDCl_3$) δ 7.60 (d, J = 8.5 Hz, 2H), 7.40 (d, J = 8.4 Hz, 2H), 6.78 (s, 1H), 5.14 (dd, J = 10.8, 6.4 Hz, 1H), 3.70 – 3.61 (m, 2H), 3.32 (dt, J = 13.6, 6.8 Hz, 1H), 3.20 (td, J = 13.1, 7.2 Hz, 1H), 1.55 – 1.49 (m, 2H), 1.34 – 1.25 (m, 5H), 0.87 (t, J = 6.9 Hz, 3H).; ^{13}C NMR (126 MHz, $CDCl_3$) δ 170.72, 157.34, 130.80, 128.88, 128.35, 127.03, 78.95, 39.74, 39.31, 31.75, 29.37, 29.18, 29.15, 26.82, 22.62, 14.08.; HRMS –QTOF MS/MS: m/z $[M+H]^+$ calcd for $C_{18}H_{27}N_2O_2$: 303.2073; found, 303.2070

5.3.17. 3-(4-fluorophenyl)-N-octyl-4,5-dihydroisoxazole-5-carboxamide (**7e**).

White solid; Yield: 85%; m.p. 92°C; ^{1}H NMR (500 MHz, $CDCl_3$) δ 7.46 – 7.35 (m, 3H), 7.19 – 7.11 (m, 1H), 6.79 (s, 1H), 5.15 (dd, J = 10.6, 6.6 Hz, 1H), 3.71 – 3.62 (m, 2H), 3.32 (td, J = 13.4, 7.1 Hz, 1H), 3.21 (td, J = 13.1, 7.2 Hz, 1H), 1.54 – 1.48 (m, 2H), 1.26 (d, J = 9.5 Hz, 10H), 0.86 (t, J = 7.0 Hz, 3H).; ^{13}C NMR (126 MHz, $CDCl_3$) δ 170.45, 163.74, 161.78, 156.52, 130.57, 122.88, 117.86, 113.89, 79.21, 39.51, 39.35, 31.73, 29.35, 29.17, 29.14, 26.81, 22.61, 14.06.; HRMS –QTOF MS/MS: m/z $[M+H]^+$ calcd for $C_{18}H_{26}N_2O_2F$: 321.1978; found, 321.1978.

5.3.18. N-cycloheptyl-3-(3-fluorophenyl)-4,5-dihydroisoxazole-5-carboxamide (**8a**).

White solid; Yield: 78%; m.p. 105°C; ^{1}H NMR (500 MHz, $CDCl_3$) δ 8.09 (dd, J = 8.1, 0.9 Hz, 1H), 7.71 (td, J = 7.5, 1.3 Hz, 1H), 7.64 (td, J = 8.0, 1.5 Hz, 1H), 7.51 (dd, J = 7.6, 1.5 Hz, 1H), 6.79 (s, 1H), 5.20 (dd, J = 11.4, 5.4 Hz, 1H), 3.69 – 3.57 (m, 2H), 3.33 (dd, J = 13.4, 7.0 Hz, 2H), 1.58 (dd, J = 14.4, 7.4 Hz, 2H), 1.39 – 1.28 (m, 5H), 0.90 (t, J = 7.0 Hz, 3H).; ^{13}C NMR (126 MHz, $CDCl_3$) δ 172.92., 168.35, 166.41, 160.98, 136.23, 128.13, 122.24, 118.61, 84.70, 55.14, 43.36, 39.34, 39.28, 32.90, 32.89, 29.01, 28.98; HRMS –QTOF MS/MS: m/z $[M+H]^+$ calcd for $C_{17}H_{22}N_2O_2F$: 305.1667; found, 305.1665.

5.3.19. N-cycloheptyl-3-(4-fluorophenyl)-4,5-dihydroisoxazole-5-carboxamide (**8b**).

White solid; Yield: 89%; m.p. 125°C; ^{1}H NMR (500 MHz, $CDCl_3$) δ 7.43 – 7.37 (m, 3H), 7.15 (ddd, J = 9.6, 4.2, 2.5 Hz, 1H), 6.73 (s, 1H), 5.13 (dd, J = 10.4, 7.1 Hz, 1H), 3.94 (dt, J = 12.9, 4.4 Hz, 1H), 3.69 – 3.63 (m, 2H), 1.97 – 1.92 (m, 1H), 1.87 – 1.82 (m, 1H), 1.61 (dd, J = 16.9, 10.0 Hz, 4H), 1.54 – 1.47 (m, 4H), 1.46 – 1.38 (m, 2H).; ^{13}C NMR (126 MHz, $CDCl_3$) δ 169.21, 163.76, 156.46, 130.56, 130.53, 122.88, 117.84, 113.90, 79.22, 50.44, 39.44, 34.97, 34.89, 27.92, 27.89, 24.06, 24.00.; HRMS –QTOF MS/MS: m/z $[M+H]^+$ calcd for $C_{17}H_{22}N_2O_2F$: 305.1667; found, 305.1664.

5.3.20. N-cycloheptyl-3-(p-tolyl)-4,5-dihydroisoxazole-5-carboxamide(**8c**).

White solid; Yield: 82%; m.p. 112°C; ^{1}H NMR (500 MHz, $CDCl_3$) δ 7.55 (d, J = 8.2 Hz, 2H), 7.22 (d, J = 8.0 Hz, 2H), 6.78 (s, 1H), 5.09 (dd, J = 9.6, 7.7 Hz, 1H), 3.93 (ddt, J = 13.0, 8.7, 4.4 Hz, 1H), 3.68 – 3.63 (m, 2H), 2.38 (s, 3H), 1.97 – 1.91 (m, 1H), 1.86 – 1.81 (m, 1H), 1.61 (ddd, J = 10.4, 6.7, 1.8 Hz, 4H), 1.50 (dd, J = 14.6, 6.9 Hz, 4H), 1.45 – 1.37 (m, 2H).; ^{13}C NMR (126 MHz, $CDCl_3$) δ 169.61, 157.19, 141.13, 129.56, 126.97, 125.57, 78.83, 50.36, 39.81, 34.96, 34.89, 27.93, 27.90, 24.07, 24.01, 21.48.; HRMS –QTOF MS/MS: m/z $[M+H]^+$ calcd for $C_{18}H_{25}N_2O_2$: 301.1916; found, 301.1915.

5.3.21. 3-(4-cyanophenyl)-N-cycloheptyl-4,5-dihydroisoxazole-5-carboxamide (**8d**).

White solid; Yield: 82%; m.p. 130°C; ^{1}H NMR (500 MHz, $CDCl_3$) δ 7.80 – 7.70 (m, 4H), 6.68 (d, J = 7.9 Hz, 1H), 5.17 (dd, J = 11.5, 6.1 Hz, 1H), 3.97 – 3.90 (m, 1H), 3.74 – 3.62 (m, 2H), 1.98 – 1.93 (m, 1H), 1.87 – 1.82 (m, 1H), 1.66 – 1.58 (m, 4H), 1.49 (dd, J = 14.0, 5.2 Hz, 4H), 1.42 (dd, J = 20.2, 9.2 Hz, 2H).;

^{13}C NMR (126 MHz, $CDCl_3$) δ 168.83, 156.06, 132.68, 132.62, 127.50, 118.12, 114.14, 79.63, 50.52, 38.91, 34.97, 34.89, 27.91, 27.87, 24.04, 23.99.; HRMS –QTOF MS/MS: m/z $[M+H]^+$ calcd for $C_{18}H_{22}N_3O_2$: 312.1712; found, 312.1710, m/z $[M+H]^+$ calcd for $C_{18}H_{22}N_3O_2$: 334.1531; found, 334.1532.

5.3.22. N-cycloheptyl-3-(4-methoxyphenyl)-4,5-dihydroisoxazole-5-carboxamide (**8e**).

White solid; Yield: 71%; m.p. 82°C; ^1H NMR (500 MHz, $CDCl_3$) δ 7.61 (d, J = 8.9 Hz, 2H), 6.93 (d, J = 8.9 Hz, 2H), 6.78 (d, J = 8.1 Hz, 1H), 5.08 (dd, J = 9.7, 7.6 Hz, 1H), 3.92 (dd, J = 8.6, 4.3 Hz, 1H), 3.67 – 3.63 (m, 2H), 1.93 (dd, J = 11.1, 3.9 Hz, 1H), 1.86 – 1.81 (m, 1H), 1.60 (dd, J = 17.2, 10.6 Hz, 4H), 1.50 (dd, J = 16.6, 8.8 Hz, 4H), 1.42 (dd, J = 11.7, 8.5 Hz, 2H).; ^{13}C NMR (126 MHz, $CDCl_3$) δ 169.68, 161.56, 156.78, 128.63, 120.89, 114.28, 78.75, 55.40, 50.36, 39.91, 34.97, 34.90, 27.94, 27.90, 24.07, 24.01.; HRMS –QTOF MS/MS: m/z $[M+H]^+$ calcd for $C_{18}H_{25}N_2O_3$: 317.1865; found, 317.1862.

5.3.23. 3-(3-nitrophenyl)-N-pentyl-4,5-dihydroisoxazole-5-carboxamide (**9a**).

White solid; Yield: 78%; m.p. 99°C; ^1H NMR (500 MHz, $CDCl_3$) δ 8.52 (t, J = 1.9 Hz, 1H), 8.30 (ddd, J = 8.2, 2.2, 1.0 Hz, 1H), 8.02 – 7.99 (m, 1H), 7.64 (t, J = 8.0 Hz, 1H), 6.78 (s, 1H), 5.22 (dd, J = 11.5, 5.7 Hz, 1H), 3.80 – 3.68 (m, 2H), 3.34 (dd, J = 13.5, 6.4 Hz, 1H), 3.22 (dt, J = 13.2, 6.5 Hz, 1H), 1.56 – 1.50 (m, 2H), 1.34 – 1.28 (m, 5H), 0.88 (t, J = 7.0 Hz, 3H).; ^{13}C NMR (126 MHz, $CDCl_3$) δ 170.08, 155.80, 148.51, 132.49, 130.23, 130.03, 125.16, 121.89, 79.58, 39.40, 39.14, 29.04, 28.96, 22.28, 13.94.; HRMS –QTOF MS/MS: m/z $[M+H]^+$ calcd for $C_{15}H_{19}N_3O_4$: 306.1454; found, 306.1450, m/z $[M+Na]^+$ calcd for $C_{15}H_{19}N_3O_4$: 328.1273; found, 328.1270.

5.3.24. 3-(4-fluorophenyl)-N-pentyl-4,5-dihydroisoxazole-5-carboxamide (**9b**).

White solid; Yield: 89%; m.p. 110°C; ^1H NMR (500 MHz, $CDCl_3$) δ 7.45 – 7.37 (m, 3H), 7.14 (dt, J = 4.6, 4.0 Hz, 1H), 6.81 (s, 1H), 5.17 (dd, J = 10.5, 6.8 Hz, 1H), 3.71 – 3.63 (m, 2H), 3.37 – 3.30 (m, 1H), 3.21 (td, J = 13.1, 7.2 Hz, 1H), 1.55 – 1.49 (m, 2H), 1.34 – 1.25 (m, 5H), 0.87 (t, J = 7.0 Hz, 3H).; ^{13}C NMR (126 MHz, $CDCl_3$) δ 170.49, 163.74, 156.51, 130.51, 130.40, 122.86, 117.70, 113.71, 79.20, 39.50, 39.34, 29.04, 28.95, 22.28, 13.93.; HRMS –QTOF MS/MS: m/z $[M+H]^+$ calcd for $C_{16}H_{19}N_3O_4F$: 279.1509; found, 279.1507.

5.3.25. 3-(4-chlorophenyl)-N-pentyl-4,5-dihydroisoxazole-5-carboxamide (**9c**).

White solid; Yield: 93%; m.p. 122°C; ^1H NMR (500 MHz, $CDCl_3$) δ 7.60 (d, J = 8.5 Hz, 2H), 7.40 (d, J = 8.4 Hz, 2H), 6.78 (s, 1H), 5.14 (dd, J = 10.8, 6.4 Hz, 1H), 3.70 – 3.61 (m, 2H), 3.32 (dt, J = 13.6, 6.8 Hz, 1H), 3.20 (td, J = 13.1, 7.2 Hz, 1H), 1.55 – 1.49 (m, 2H), 1.34 – 1.25 (m, 5H), 0.87 (t, J = 6.9 Hz, 3H).; ^{13}C NMR (126 MHz, $CDCl_3$) δ 170.48, 156.46, 136.85, 129.18, 128.25, 126.86, 79.14, 39.49, 39.31,

29.04, 28.95, 22.28, 13.93.; HRMS –QTOF MS/MS: m/z $[M+H]^+$ calcd for $C_{16}H_{19}N_3O_4Cl$: 295.1213; found, 295.1210.

5.3.26. 3-(2-nitrophenyl)-N-pentyl-4,5-dihydroisoxazole-5-carboxamide (**9d**).

White solid; Yield: 72%; m.p. 115°C; ^{1}H NMR (500 MHz, $CDCl_3$) δ 8.09 (dd, J = 8.1, 0.9 Hz, 1H), 7.71 (td, J = 7.5, 1.3 Hz, 1H), 7.64 (td, J = 8.0, 1.5 Hz, 1H), 7.51 (dd, J = 7.6, 1.5 Hz, 1H), 6.79 (s, 1H), 5.20 (dd, J = 11.4, 5.4 Hz, 1H), 3.69 – 3.57 (m, 2H), 3.33 (dd, J = 13.4, 7.0 Hz, 2H), 1.58 (dd, J = 14.4, 7.4 Hz, 2H), 1.39 – 1.28 (m, 5H), 0.90 (t, J = 7.0 Hz, 3H).; ^{13}C NMR (126 MHz, $CDCl_3$) δ 170.20, 156.36, 133.53, 131.08, 130.72, 125.00, 124.45, 79.46, 42.37, 39.38, 29.10, 28.98, 22.33, 13.97.; HRMS –QTOF MS/MS: m/z $[M+H]^+$ calcd for $C_{15}H_{19}N_3O_4$: 306.1454; found, 306.1452.

5.3.27. N-butyl-3-(4-fluorophenyl)-4,5-dihydroisoxazole-5-carboxamide (**10a**).

White solid; Yield: 87%; m.p. 99°C; ^{1}H NMR (500 MHz, $CDCl_3$) δ 7.44 – 7.38 (m, 3H), 7.17 – 7.12 (m, 1H), 6.76 (s, 1H), 5.15 (dd, J = 10.6, 6.7 Hz, 1H), 3.70 – 3.63 (m, 2H), 3.34 (td, J = 13.5, 7.0 Hz, 1H), 3.22 (dt, J = 13.2, 6.5 Hz, 1H), 1.53 – 1.47 (m, 2H), 1.36 – 1.32 (m, 2H), 0.91 (t, J = 7.3 Hz, 3H).; ^{13}C NMR (126 MHz, $CDCl_3$) δ 170.45, 163.74, 156.51, 130.53, 130.38, 122.87, 117.90, 113.90, 79.19, 39.49, 39.06, 31.41, 20.00, 14.15, 13.70.; HRMS –QTOF MS/MS: m/z $[M+H]^+$ calcd for $C_{14}H_{18}N_2O_2F$: 265.1352; found, 265.1347.

5.3.28. N-butyl-3-(3-fluorophenyl)-4,5-dihydroisoxazole-5-carboxamide (**10b**).

White solid; Yield: 83%; m.p. 109°C; ^{1}H NMR (500 MHz, $CDCl_3$) δ 7.44 – 7.37 (m, 3H), 7.15 (ddd, J = 9.4, 6.5, 2.5 Hz, 1H), 6.77 (brs, 1H), 5.15 (dd, J = 10.6, 6.7 Hz, 1H), 3.70 – 3.62 (m, 2H), 3.33 (dt, J = 13.5, 6.7 Hz, 1H), 3.25 – 3.18 (m, 1H), 1.50 (ddd, J = 14.6, 10.0, 4.9 Hz, 2H), 1.34 (dd, J = 15.1, 7.4 Hz, 2H), 0.91 (t, J = 7.3 Hz, 3H).; ^{13}C NMR (126 MHz, $CDCl_3$) δ 170.45, 163.74, 156.53, 130.52, 130.39, 122.87, 117.72, 113.72, 79.19, 39.48, 39.05, 31.41, 20.00, 13.70.; HRMS –QTOF MS/MS: m/z $[M+H]^+$ calcd for $C_{14}H_{18}N_2O_2F$: 265.1352; found, 265.1347.

5.3.29. N-butyl-3-(3-nitrophenyl)-4,5-dihydroisoxazole-5-carboxamide (**10c**).

White solid; Yield: 80%; m.p. 63°C; ^{1}H NMR (500 MHz, $CDCl_3$) δ 8.51 (s, 1H), 8.3 – 8.27 (m, 1H), 8.01 (d, J = 0.5 Hz, 1H), 7.63 (t, J = 8.0 Hz, 1H), 6.75 (s, 1H), 5.22 (dd, J = 11.6, 5.7 Hz, 1H), 3.75 (dq, J = 17.2, 5.7 Hz, 2H), 3.34 (dt, J = 13.6, 6.7 Hz, 1H), 3.23 (dt, J = 13.6, 6.7 Hz, 1H), 1.51 (dd, J = 15.0, 7.6 Hz, 2H), 1.35 (dd, J = 15.0, 7.6 Hz, 2H), 0.92 (t, J = 7.3 Hz, 3H).; ^{13}C NMR (126 MHz, $CDCl_3$) δ 170.08, 155.80, 148.51, 132.50, 130.22, 130.04, 125.18, 121.91, 79.57, 39.13, 31.40, 20.01, 13.70.; HRMS –QTOF MS/MS: m/z $[M+H]^+$ calcd for $C_{14}H_{18}N_3O_4$: 292.1297; found, 292.1295.

5.3.30. 3-(4-bromophenyl)-N-butyl-4,5-dihydroisoxazole-5-carboxamide (**10d**).

White solid; Yield: 86%; m.p. 65°C; ^{1}H NMR (500 MHz, $CDCl_3$) δ 7.54 (q, J = 8.8 Hz, 4H), 6.77 (s, 1H), 5.14 (dd, J = 10.8, 6.4 Hz, 1H), 3.66 (dd, J = 8.6, 5.7 Hz, 2H), 3.33 (dt, J = 13.5, 6.7 Hz, 1H), 3.25 – 3.18 (m, 1H), 1.53 – 1.47 (m, 2H), 1.36 – 1.32 (m, 2H), 0.91 (t, J = 7.4 Hz, 3H).; ^{13}C NMR (126 MHz, $CDCl_3$) δ 170.49, 156.56, 132.15, 128.45, 127.28, 125.21, 79.15, 39.42, 39.05, 31.41, 20.00, 13.70.; HRMS – QTOF MS/MS: m/z $[M+H]^+$ calcd for $C_{14}H_{18}N_2O_2Br$: 325.0552; found, 325.0551.

5.3.31. N-butyl-3-(3-chlorophenyl)-4,5-dihydroisoxazole-5-carboxamide (**10e**).

White solid; Yield: 88%; m.p. 81°C; ^{1}H NMR (500 MHz, $CDCl_3$) δ 7.68 (t, J = 1.8 Hz, 1H), 7.54 – 7.51 (m, 1H), 7.42 (ddd, J = 8.0, 2.0, 1.1 Hz, 1H), 7.36 (t, J = 7.9 Hz, 1H), 6.76 (s, 1H), 5.15 (dd, J = 10.9, 6.3 Hz, 1H), 3.70 – 3.61 (m, 2H), 3.34 (dd, J = 13.5, 6.4 Hz, 1H), 3.21 (dd, J = 13.5, 5.9 Hz, 1H), 1.53 – 1.48 (m, 2H), 1.34 (d, J = 7.6 Hz, 2H), 0.91 (t, J = 7.3 Hz, 3H).; ^{13}C NMR (126 MHz, $CDCl_3$) δ 170.43, 156.38, 134.96, 130.78, 130.16, 130.09, 127.02, 125.14, 79.18, 39.40, 39.07, 31.41, 20.00, 13.70.; HRMS – QTOF MS/MS: m/z $[M+Na]^+$ calcd for $C_{14}H_{18}N_2O_2Cl$: 303.0806; found, 303.0807.

5.3.32. N-cyclopropyl-3-(3-nitrophenyl)-4,5-dihydroisoxazole-5-carboxamide (**11a**).

White solid; Yield: 83%; m.p. 92°C; ^{1}H NMR (500 MHz, $CDCl_3$) δ 8.51 (t, J = 1.7 Hz, 1H), 8.30 (d, J = 9.6 Hz, 1H), 8.00 (d, J = 7.8 Hz, 1H), 7.64 (t, J = 8.0 Hz, 1H), 6.83 (s, 1H), 5.20 (dd, J = 11.7, 5.6 Hz, 1H), 3.74 (ddd, J = 29.0, 17.3, 8.7 Hz, 2H), 2.76 (tq, J = 7.4, 3.8 Hz, 1H), 0.85 – 0.78 (m, 2H), 0.62 – 0.52 (m, 2H).; ^{13}C NMR (126 MHz, $CDCl_3$) δ 171.59, 155.76, 148.52, 132.50, 130.16, 130.04, 125.19, 121.91, 79.54, 39.08, 22.45, 6.46, 6.37.; HRMS –QTOF MS/MS: m/z $[M+H]^+$ calcd for $C_{13}H_{13}N_3O_4$: 276.0984; found, 276.0979.

5.3.33. N-cyclopropyl-3-(4-fluorophenyl)-4,5-dihydroisoxazole-5-carboxamide (**11b**).

White solid; Yield: 78%; m.p. 93°C; ^{1}H NMR (500 MHz, $CDCl_3$) δ 7.45 – 7.39 (m, 3H), 7.20 – 7.13 (m, 1H), 6.85 (s, 1H), 5.15 (dd, J = 11.2, 6.2 Hz, 1H), 3.73 – 3.63 (m, 2H), 2.76 (tq, J = 7.4, 3.8 Hz, 1H), 0.85 – 0.78 (m, 2H), 0.61 – 0.53 (m, 2H).; ^{13}C NMR (126 MHz, $CDCl_3$) δ 171.98, 163.75, 156.49, 130.60, 130.39, 122.90, 117.92, 113.91, 79.15, 39.42, 22.39, 6.43, 6.35.; HRMS –QTOF MS/MS: m/z $[M+H]^+$ calcd for $C_{13}H_{13}N_2O_2F$: 249.1039; found, 249.1034.

5.3.34. 3-(4-bromophenyl)-N-cyclopropyl-4,5-dihydroisoxazole-5-carboxamide (**11c**).

White solid; Yield: 82%; m.p. 114°C; ^{1}H NMR (500 MHz, $CDCl_3$) δ 7.54 (q, *J* = 8.6 Hz, 4H), 6.84 (s, 1H), 5.12 (dd, J = 11.1, 5.8 Hz, 1H), 3.74 – 3.58 (m, 2H), 2.75 (dt, J = 10.6, 3.5 Hz, 1H), 0.83 – 0.75 (m, 2H), 0.55 (dt, J = 13.9, 11.6 Hz, 2H).; ^{13}C NMR (126 MHz, $CDCl_3$) δ 172.10, 156.54, 132.16, 128.46, 127.20,

125.25, 79.10, 39.37, 22.40, 6.44.; HRMS –QTOF MS/MS: m/z $[M+H]^+$ calcd for $C_{13}H_{14}N_2O_2$: 309.0239; found, 309.0234.

5.3.35. 3-(4-chlorophenyl)-N-cyclopropyl-4,5-dihydroisoxazole-5-carboxamide (**11d**).

White solid; Yield: 92%; m.p. 75°C; ^{1}H NMR (500 MHz, $CDCl_3$) δ 7.68 (s, 1H), 7.52 (d, J = 7.4 Hz, 1H), 7.42 (d, J = 7.6 Hz, 1H), 7.36 (t, J = 7.8 Hz, 1H), 6.85 (s, 1H), 5.13 (dd, J = 11.0, 5.8 Hz, 1H), 3.73 – 3.60 (m, 2H), 2.75 (d, J = 3.3 Hz, 1H), 0.80 (d, J = 5.9 Hz, 2H), 0.55 (d, J = 13.9 Hz, 2H).; ^{13}C NMR (126 MHz, $CDCl_3$) δ 171.99, 156.34, 134.96, 130.80, 130.17, 130.03, 127.02, 125.15, 79.15, 39.35, 22.41, 6.43, 6.35.; HRMS –QTOF MS/MS: m/z $[M+H]^+$ calcd for $C_{13}H_{14}N_2O_2Cl$: 265.0744; found, 265.0740.

5.3.36. 3-(4-(benzyloxy)phenyl)-N-cyclopropyl-4,5-dihydroisoxazole-5-carboxamide (**11e**).

White solid; Yield: 67%; m.p. 98°C; ^{1}H NMR (500 MHz, $CDCl_3$) δ 7.62 – 7.57 (m, 2H), 7.41 (dt, J = 14.7, 4.6 Hz, 4H), 7.36 – 7.32 (m, 1H), 7.03 – 6.97 (m, 2H), 6.85 (s, 1H), 5.11 (s, 2H), 5.06 (dd, J = 11.0, 6.1 Hz, 1H), 3.70 – 3.60 (m, 2H), 2.73 (tq, J = 7.4, 3.8 Hz, 1H), 0.83 – 0.74 (m, 2H), 0.59 – 0.49 (m, 2H).; ^{13}C NMR (126 MHz, $CDCl_3$) δ 172.44, 160.74, 156.80, 136.33, 128.70, 128.67, 128.21, 127.46, 120.98, 115.21, 78.70, 70.10, 39.88, 22.34, 6.41, 6.32. HRMS –QTOF MS/MS: m/z $[M+Na]^+$ calcd for $C_{20}H_{21}N_2O_3$: 359.1372; found, 359.1369.

5.3.37. N-(6-methoxybenzo[d]thiazol-2-yl)-3-phenyl-4,5-dihydroisoxazole-5-carboxamide (**12a**)

White solid; Yield: 68%; m.p. 123°C; ^{1}H NMR (500 MHz, DMSO-D_6) δ 12.64 (s, 1H), 7.75 – 7.73 (m, 2H), 7.70 – 7.68 (d, 1H), 7.60 – 7.60 (d, 1H), 7.50 (d, 2H), 7.49 (d, 1H), 7.07 – 7.05 (dd, 1H), 5.45 (t, 1H), 3.82 (s, 3H), 3.79 (d, 2H). . HRMS –QTOF MS/MS: m/z $[M+H]^+$ calcd for $C_{18}H_{15}N_3O_3S$: 354.0912; found, 354.0914.

5.3.38. 3-(3-fluorophenyl)-N-(6-methoxybenzo[d]thiazol-2-yl)-4,5-dihydroisoxazole-5-carboxamide **(12b)**

White solid; Yield: 86%; m.p. 154°C; ^{1}H NMR (500 MHz, DMSO-D_6) δ 12.69 (s, 1H), 7.70 – 7.68 (d, 1H), 7.61 – 7.54 (m, 4H), 7.37 (t, 1H), 7.07 (d, 1H), 5.48 (t, 1H), 3.82 (s, 3H), 3.80 (d, 2H); ^{13}C NMR (126 MHz, DMSO-D_6) δ 168.80, 163.61, 161.67, 156.84, 156.44, 143.09, 133.41, 131.48, 131.23, 123.59, 121.87, 117.66, 115.61, 113.93, 105.26, 79.40, 56.12, 38.37. HRMS –QTOF MS/MS: m/z $[M+H]^+$ calcd for $C_{18}H_{14}N_3O_3SF$: 372.0818; found, 372.0820.

5.3.39. 3-(3-chlorophenyl)-N-(6-methoxybenzo[d]thiazol-2-yl)-4,5-dihydroisoxazole-5-carboxamide **(12c)**

White solid; Yield: 82%; m.p. 145°C; ^{1}H NMR (500 MHz, DMSO-D_6) δ 12.61 (s, 1H), 7.69 (d, 1H), 7.63 – 7.61 (m, 2H), 7.54 – 7.44 (m, 3H), 6.98 (dd, 1H), 5.40 (t, 1H), 3.75 (s, 3H), 3.72 (d, 2H); ^{13}C NMR (126 MHz, DMSO-D_6) δ 168.81, 156.83, 156.32, 155.90, 143.07, 134.12, 133.40, 131.29, 131.08, 130.69, 126.98, 126, 121.85, 115.60, 105.26, 79.43, 56.12, 38.29. HRMS –QTOF MS/MS: m/z $[M+H]^+$ calcd for $C_{18}H_{14}N_3O_3SCl$: 388.0523; found, 388.0525.

5.3.40. 3-(4-fluorophenyl)-N-(6-methoxybenzo[d]thiazol-2-yl)-4,5-dihydroisoxazole-5-carboxamide **(12d)**

White solid; Yield: 92%; m.p. 169°C; ^{1}H NMR (500 MHz, DMSO-D_6) δ 12.70 (s, 1H), 7.70 (d, 1H), 7.61 – 7.54 (m, 4H), 7.36 (t, 1H), 7.07 (d, 1H), 5.48 (t, 1H), 3.82 (s, 3H), 3.80 (d, 2H); ^{13}C NMR (126 MHz, DMSO-D_6) δ 168.83, 163.60, 161.66, 156.82, 156.45, 155.92, 143.01, 133.39, 131.49, 123.62, 121.85, 117.84, 115.61, 105.23, 79.39, 56.11, 38.36.; HRMS –QTOF MS/MS: m/z $[M+H]^+$ calcd for $C_{18}H_{14}N_3O_3SF$: 372.0818; found, 372.0821.

5.4. Antibiotic susceptibility testing against mycobacteria

Antimycobacterial susceptibility testing was carried out on newly synthesized compounds by using broth microdilution assay.[30, 31] 10 mg/mL stock solutions of test and control compounds were prepared in DMSO and stored in -20˚C. Mycobacterial cultures were inoculated in Middlebrook 7H9 enriched (Difco, Becton, NJ, USA) media supplemented with 10% ADC-Tween-80 (Bovine Serum Albumin, Dextrose, 0.2% glycerol and 0.05% Tween-80) and OD_{600} of cultures was measured, followed by dilution to achieve ~10^6 cfu/mL. [32] The newly synthesized compounds were tested from 64-0.5 mg/L in two-fold serial diluted fashion with 2.5 µL of each concentration added per well of a 96-well round bottom microtitre plate. Later, 97.5 µL of bacterial suspension was added to each well containing the test compound along with appropriate controls. Presto blue (Thermo Fisher, USA) resazurin-based dye was used for the visualized identification of active compounds. MIC of active compound was determined as lowest concentration of compound that inhibited visible growth after incubation period. For each compound, MIC determinations were replicated thrice using duplicate samples. The MIC plates were incubated at 37˚C for 7 days for Mtb and 48 hr for other mycobacterial pathogens.

5.5. Antibiotic susceptibility testing against ESKAPE pathogen panel

Antibiotic susceptibility testing was carried out on the newly synthesized compounds by determining the Minimum Inhibitory Concentration (MIC) with reference to the standard CLSI guidelines.[33, 34] MIC is defined as the minimum concentration of compound at which visible bacterial growth is

inhibited. Bacterial cultures were grown in Mueller-Hinton cation supplemented broth (CAMHB). Optical density (OD_{600}) of the cultures was measured, followed by dilution for ~10^6 cfu/mL. This inoculum was added into a series of test wells in a microtiter plate that contained various concentrations of compound under test ranging from 64 to 0.03 mg/mL. Controls i.e., cells alone and media alone (without compound + cells) and levofloxacin used as a reference standard. Plates were incubated at 37˚C for 16-18 h followed by observations of MIC values by the absence or presence of visible growth. For each compound, MIC determinations were performed independently thrice using duplicate samples each time.

5.6. Cell cytotoxicity assay

The active newly synthesized compounds were screened for their cell toxicity against Vero cells using MTT assay.[35] ~10^3 cells/ well were seeded in 96 well plate and incubated at 37°C with a 5% CO_2 atmosphere. After 24 h, compound was added ranging from 100 to 5 mg/L and incubated for 72 h at 37°C with 5% CO_2 atmosphere. After the incubation was over, MTT was added at 5 mg/L in each well, incubated at 37°C for further 4 h, residual medium was discarded, 0.1 mL of DMSO was added to solubilise the formazan crystals and OD was taken at 540 nm for the calculation of CC_{50}. CC_{50} is defined as the lowest concentration of compound which leads to a 50% reduction in cell viability. Doxorubicin was used as positive control and each experiment was repeated in triplicate.

CRediT author statement.

Nikhil Baliram Gaikwad: Writing - Original Draft, Conceptualization, Investigation, Methodology, Software, Visualization.

Pathan Afroz: Methodology

Mohammad Naiyaz Ahmad: Methodology, Investigation.

Grace Kaul: Writing - Review & Editing,

Manjulika Shukla: Writing - Review & Editing,

Srinivas Nanduri: Writing - Review & Editing,

Arunava Dasgupta: Writing - Review & Editing,

Sidharth Chopra: Supervision, Writing - Review & Editing

Venkata Madhavi Yaddanapudi: Supervision, Writing - Review & Editing, Project administration

All the authors of this manuscript Nikhil Baliram Gaikwad, Pathan Afroz, Mohammad Naiyaz Ahmad , Grace Kaul, Manjulika Shukla, Srinivas Nanduri, Arunava Dasgupta, Sidharth Chopra and Venkata Madhavi Yaddanapudi declare that are no conflicts of interest

Conflicts of interest

All the authors declare no conflicts of interest.

Acknowledgements

NG and YVM thank and acknowledge the Department of Pharmaceuticals, Ministry of Chemicals & Fertilizers, Govt. of India, for the award of NIPER fellowship. MN thanks CSIR, GK thanks DST-INSPIRE and MS thanks UGC for their fellowship. The manuscript has the NIPER Research Communication No.-NIPER-H/2020/0M6.

References

[1] WHO, tuberculosis, https://www.who.int/tb/strategy/end-tb/en/.(accessed on 3 feb 2020).
[2] W.H. Organization, The end TB strategy, World Health Organization, 2015.
[3] M. Uplekar, D. Weil, K. Lonnroth, E. Jaramillo, C. Lienhardt, H.M. Dias, D. Falzon, K. Floyd, G. Gargioni, H. Getahun, WHO's new end TB strategy, The Lancet 385(9979) (2015) 1799-1801.
[4] I. Epstein, K. Nair, L. Boyd, Cycloserine, a new antibiotic, in the treatment of human pulmonary tuberculosis: a preliminary report, Antibiotic Med. 1(2) (1955) 80-93.
[5] C.A. Desjardins, K.A. Cohen, V. Munsamy, T. Abeel, K. Maharaj, B.J. Walker, T.P. Shea, D.V. Almeida, A.L. Manson, A. Salazar, Genomic and functional analyses of Mycobacterium tuberculosis strains implicate ald in D-cycloserine resistance, Nature genetics 48(5) (2016) 544-551.
[6] R.P. Tangallapally, D. Sun, Rakesh, N. Budha, R.E.B. Lee, A.J.M. Lenaerts, B. Meibohm, R.E. Lee, Discovery of novel isoxazolines as anti-tuberculosis agents, Bioorganic & Medicinal Chemistry Letters 17(23) (2007) 6638-6642.
[7] Rakesh, D. Sun, R.B. Lee, R.P. Tangallapally, R.E. Lee, Synthesis, optimization and structure–activity relationships of 3,5-disubstituted isoxazolines as new anti-tuberculosis agents, European Journal of Medicinal Chemistry 44(2) (2009) 460-472.
[8] V.M. Reddy, K.R. Reddy, Synthesis and biological evaluation of some novel-3-(5-substituted benzimidazol-2-yl)-5-arylisoxazolines, Chinese Chemical Letters 21(10) (2010) 1145-1148.
[9] G.G. Mandawad, R.D. Kamble, S.V. Hese, R.A. More, R.N. Gacche, K.M. Kodam, B.S. Dawane, An efficient synthesis of isoxazoline libraries of thiophene analogs and its

antimycobacterial investigation, Medicinal Chemistry Research 23(10) (2014) 4455-4463.

[10] V.P.P. Viswajanani J. Sattigeri, Ajay Soni, Keshav Prabhakar Naik, Abhijit Ray, Sunanda G. Dastidar, Heterocyclic derivatives as cell adhesion inhibitors, WO2006090234A1 (2006).

[11] S. Bhakta, N. Scalacci, A. Maitra, A.K. Brown, S. Dasugari, D. Evangelopoulos, T.D. McHugh, P.N. Mortazavi, A. Twist, E. Petricci, F. Manetti, D. Castagnolo, Design and Synthesis of 1-((1,5-Bis(4-chlorophenyl)-2-methyl-1H-pyrrol-3-yl)methyl)-4-methylpiperazine (BM212) and N-Adamantan-2-yl-N'-((E)-3,7-dimethylocta-2,6-dienyl)ethane-1,2-diamine (SQ109) Pyrrole Hybrid Derivatives: Discovery of Potent Antitubercular Agents Effective against Multidrug-Resistant Mycobacteria, Journal of Medicinal Chemistry 59(6) (2016) 2780-2793.

[12] P. Liu, Y. Yang, Y. Ju, Y. Tang, Z. Sang, L. Chen, T. Yang, Q. An, T. Zhang, Y. Luo, Design, synthesis and biological evaluation of novel pyrrole derivatives as potential ClpP1P2 inhibitor against Mycobacterium tuberculosis, Bioorganic Chemistry 80 (2018) 422-432.

[13] R.D. Wavhale, E.A.F. Martis, P.K. Ambre, B. Wan, S.G. Franzblau, K.R. Iyer, K. Raikuvar, K. Macegoniuk, Ł. Berlicki, S.R. Nandan, E.C. Coutinho, Discovery of new leads against Mycobacterium tuberculosis using scaffold hopping and shape based similarity, Bioorganic & Medicinal Chemistry 25(17) (2017) 4835-4844.

[14] J.T. Williams, E.R. Haiderer, G.B. Coulson, K.N. Conner, E. Ellsworth, C. Chen, N. Alvarez-Cabrera, W. Li, M. Jackson, T. Dick, R.B. Abramovitch, Identification of New MmpL3 Inhibitors by Untargeted and Targeted Mutant Screens Defines MmpL3 Domains with Differential Resistance, Antimicrobial Agents and Chemotherapy 63(10) (2019) e00547-19.

[15] B. Zhang, J. Li, X. Yang, L. Wu, J. Zhang, Y. Yang, Y. Zhao, L. Zhang, X. Yang, X. Yang, X. Cheng, Z. Liu, B. Jiang, H. Jiang, L.W. Guddat, H. Yang, Z. Rao, Crystal Structures of Membrane Transporter MmpL3, an Anti-TB Drug Target, Cell 176(3) (2019) 636-648.e13.

[16] O.K. Onajole, M. Pieroni, S.K. Tipparaju, S. Lun, J. Stec, G. Chen, H. Gunosewoyo, H. Guo, N.C. Ammerman, W.R. Bishai, A.P. Kozikowski, Preliminary Structure–Activity Relationships and Biological Evaluation of Novel Antitubercular Indolecarboxamide Derivatives Against Drug-Susceptible and Drug-Resistant Mycobacterium tuberculosis Strains, Journal of Medicinal Chemistry 56(10) (2013) 4093-4103.

[17] J. Stec, O.K. Onajole, S. Lun, H. Guo, B. Merenbloom, G. Vistoli, W.R. Bishai, A.P. Kozikowski, Indole-2-carboxamide-based MmpL3 Inhibitors Show Exceptional Antitubercular Activity in an Animal Model of Tuberculosis Infection, Journal of Medicinal Chemistry 59(13) (2016) 6232-6247.

[18] S.S. Alsayed, S. Lun, G. Luna, C.C. Beh, A.D. Payne, N. Foster, W.R. Bishai, H. Gunosewoyo, Design, synthesis, and biological evaluation of novel arylcarboxamide derivatives as anti-tubercular agents, RSC Advances 10(13) (2020) 7523-7540.

[19] M. Baláž, Z. Kudličková, M. Vilková, J. Imrich, Ľ. Balážová, N. Daneu, Mechanochemical Synthesis and Isomerization of N-Substituted Indole-3-carboxaldehyde Oximes, Molecules 24(18) (2019) 3347.

[20] A. Lachman, Benzophenone oxime, Organic Syntheses (2003) 70-70.

[21] B.C. Lemercier, J.G. Pierce, Synthesis of Thiohydroxamic Acids and Thiohydroximic Acid Derivatives, The Journal of Organic Chemistry 79(5) (2014) 2321-2330.

[22] A.F. Tominey, J. Liese, S. Wei, K. Kowski, T. Schrader, A. Kraft, RAFT polymers for protein recognition, Beilstein Journal of Organic Chemistry 6 (2010) 66.

[23] L.A. Bateman, T.B. Nguyen, A.M. Roberts, D.K. Miyamoto, W.M. Ku, T.R. Huffman, Y. Petri, M.J. Heslin, C.M. Contreras, C.F. Skibola, J.A. Olzmann, D.K. Nomura, Chemoproteomics-enabled covalent ligand screen reveals a cysteine hotspot in reticulon 4 that impairs ER morphology and cancer pathogenicity, Chemical Communications 53(53) (2017) 7234-7237.

[24] J. de Ruyck, C. Dupont, E. Lamy, V. Le Moigne, C. Biot, Y. Guérardel, J.-L. Herrmann, M. Blaise, S. Grassin-Delyle, L. Kremer, F. Dubar, Structure-Based Design and Synthesis of Piperidinol-Containing Molecules as New Mycobacterium abscessus Inhibitors, ChemistryOpen 9(3) (2020) 351-365.

[25] F. Ntie-Kang, An in silico evaluation of the ADMET profile of the StreptomeDB database, SpringerPlus 2(1) (2013) 353.

[26] D.E. Clark, S.D. Pickett, Computational methods for the prediction of 'drug-likeness', Drug discovery today 5(2) (2000) 49-58.

[27] O. Ursu, A. Rayan, A. Goldblum, T. Oprea, Wiley Interdiscip, Rev.: Comput. Mol. Sci 1 (2011) 760.

[28] G.R. Bickerton, G.V. Paolini, J. Besnard, S. Muresan, A.L. Hopkins, Quantifying the chemical beauty of drugs, Nature chemistry 4(2) (2012) 90-98.

[29] C.A. Lipinski, Lead-and drug-like compounds: the rule-of-five revolution, Drug Discovery Today: Technologies 1(4) (2004) 337-341.

[30] M. Pandey, A.K. Singh, R. Thakare, S. Talwar, P. Karaulia, A. Dasgupta, S. Chopra, A.K. Pandey, Diphenyleneiodonium chloride (DPIC) displays broad-spectrum bactericidal activity, Scientific reports 7(1) (2017) 1-8.

[31] I. Wiegand, K. Hilpert, R.E.W. Hancock, Agar and broth dilution methods to determine the minimal inhibitory concentration (MIC) of antimicrobial substances, Nature Protocols 3(2) (2008) 163-175.

[32] T. Štular, S. Lešnik, K. Rožman, J. Schink, M. Zdouc, A. Ghysels, F. Liu, C.C. Aldrich, V.J. Haupt, S. Salentin, Discovery of mycobacterium tuberculosis InhA inhibitors by binding sites comparison and ligands prediction, Journal of medicinal chemistry 59(24) (2016) 11069-11078.

[33] J.H. Jorgensen, J.F. Hindler, L.B. Reller, M.P. Weinstein, New Consensus Guidelines from the Clinical and Laboratory Standards Institute for Antimicrobial Susceptibility Testing of Infrequently Isolated or Fastidious Bacteria, Clinical Infectious Diseases 44(2) (2007) 280-286.

[34] P. Wayne, CLSI document M07-A9, Clinical and Laboratory Standards Institute Standard, Approved 9th Edition (2012).

[35] S. Patel, N. Gheewala, A. Suthar, A. Shah, In-vitro cytotoxicity activity of Solanum nigrum extract against Hela cell line and Vero cell line, International journal of pharmacy and pharmaceutical sciences 1.1 (2009) 38-46.

Figure 1: Previous reports on isoxazoline scaffold and amide conjugate with anti-TB activity.

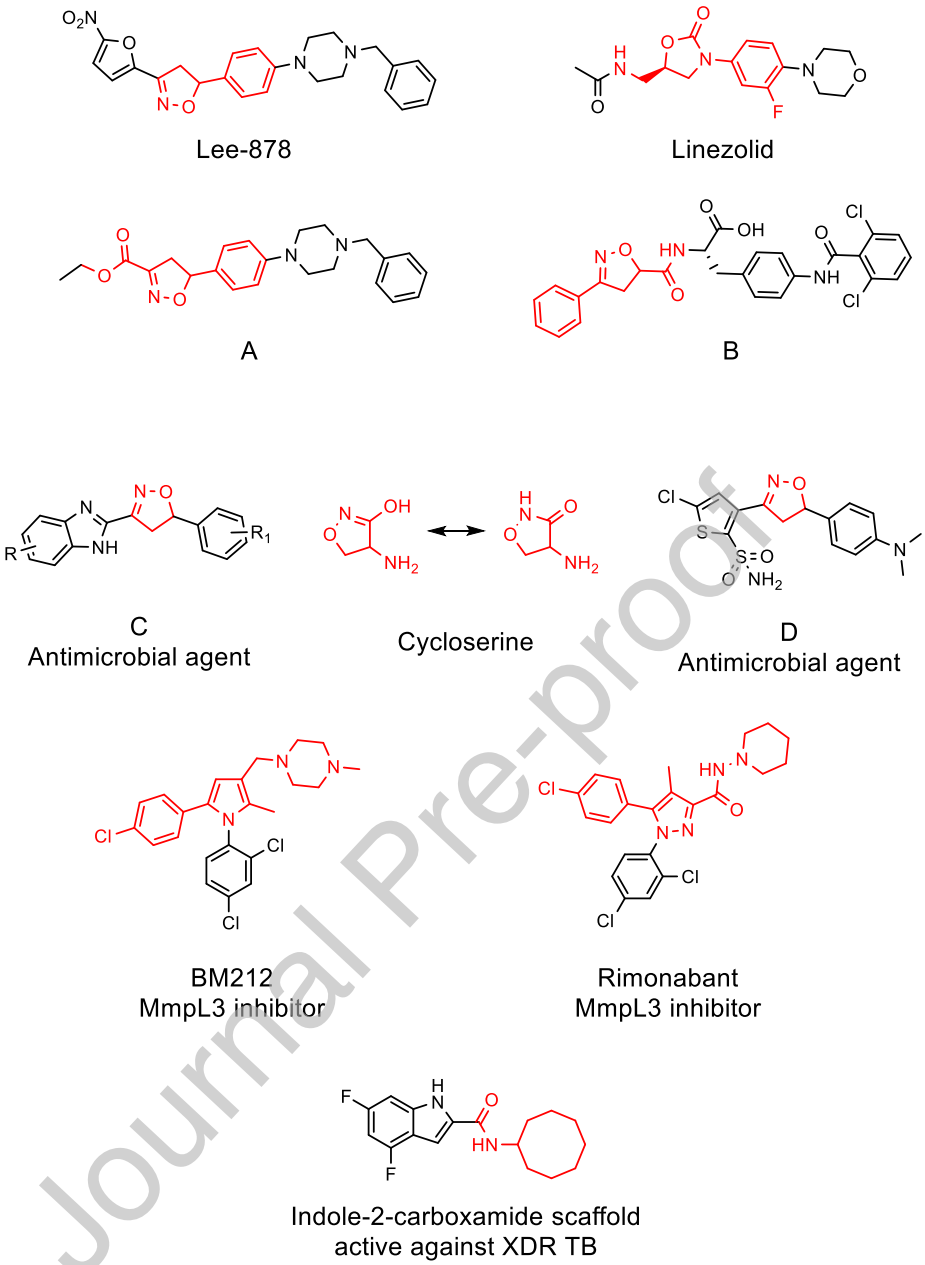

Figure 2: Superimposition of Isoxazoline hybrid derivative **6k** with BM212 and Rimonabant.

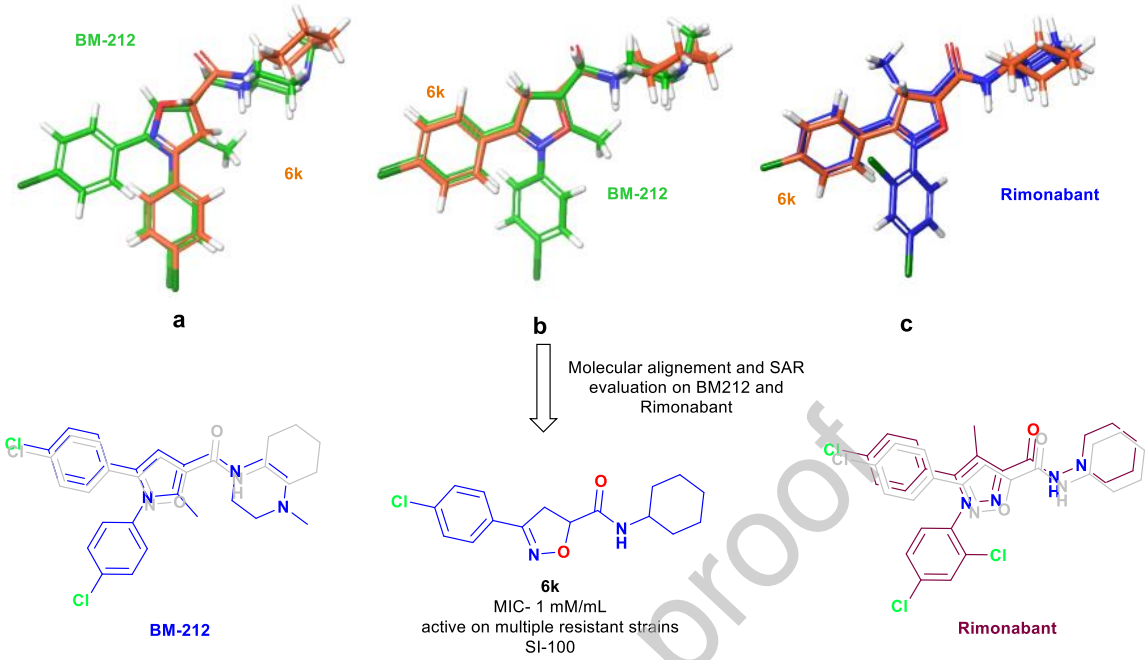

Scheme 1: Synthetic route to isoxazoline amide compounds.

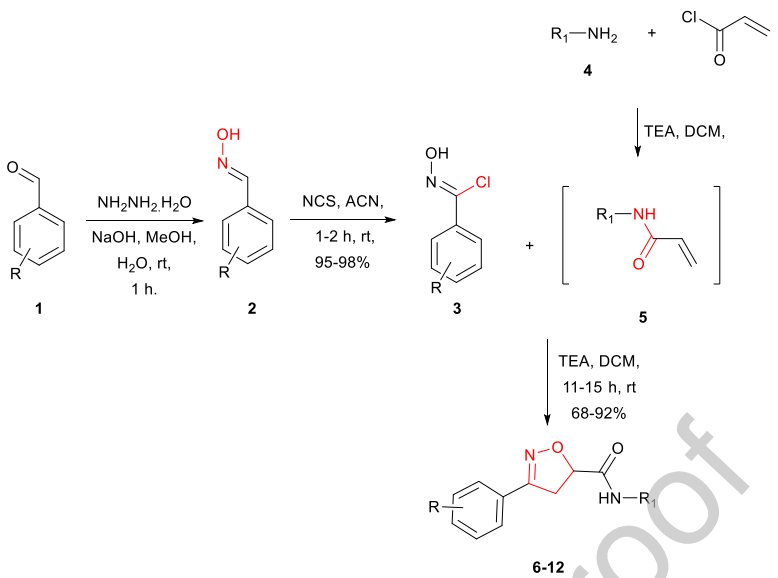

6a : R_1- Cyclohexyl, R- 2-NO_2,	7a :R1- Octyl, R- 3-Cl,	9a :R_1- Pentyl, R- 3-NO_2,	11a :R_1- Cyclopropyl, R- 3-NO_2,
6b : R_1- Cyclohexyl, R- 3-Cl,	7b :R1- Octyl, R- 4-Br,	9b :R_1- Pentyl, R- 4-F,	11b :R_1- Cyclopropyl, R- 4-F,
6c : R_1- Cyclohexyl, R- 4-Me,	7c :R1- Octyl, R- 3-F,	9c :R_1- Pentyl, R- 4-Cl,	11c :R_1- Cyclopropyl, R- 4-Br,
6d : R_1- Cyclohexyl, R- 4-CN,	7d :R1- Octyl, R- Ph,	9d :R_1- Pentyl, R- 2-NO_2.	11d :R_1- Cyclopropyl, R- 4-Cl,
6e : R_1- Cyclohexyl, R- 4-Br,	7e :R1- Octyl, R- 4-F.		11e :R_1- Cyclopropyl, R- 4(4-Benzyloxy)phenyl.
6f : R_1- Cyclohexyl, R- 4-F,			
6g : R_1- Cyclohexyl, R- 3-F,			
6h : R_1- Cyclohexyl, R- 4-NO_2,	8a :R1- Cycloheptyl, R- 3-F,	10a :R_1- Butyl, R- 4-F,	12a :R_1- 6-OMe-2-Aminobenzothiazole, R- Ph,
6i : R_1- Cyclohexyl, R- Ph,	8b :R1- Cycloheptyl, R- 4-F,	10b :R_1- Butyl, R- 3-F,	12b :R_1- 6-OMe-2-Aminobenzothiazole, R- 3-F
6j : R_1- Cyclohexyl, R- 3-NO_2,	8c :R1- Cycloheptyl, R- 4-Me,	10c :R_1- Butyl, R- 3-NO_2,	12c :R_1- 6-OMe-2-Aminobenzothiazole, R- 3-Cl,
6k : R_1- Cyclohexyl, R- 4-Cl,	8d :R1- Cycloheptyl, R- 4-CN,	10d :R_1- Butyl, R- 4-Br,	12d :R_1- 6-OMe-2-Aminobenzothiazole, R- 4-F,
6l : R_1- Cyclohexyl, R- 4-OH.	8e :R1- Cycloheptyl, R- 4-OMe.	10e :R_1- Butyl, R- 3-Cl.	

Figure 3: Correlation between MIC and CLogP values of isoxazoline series.

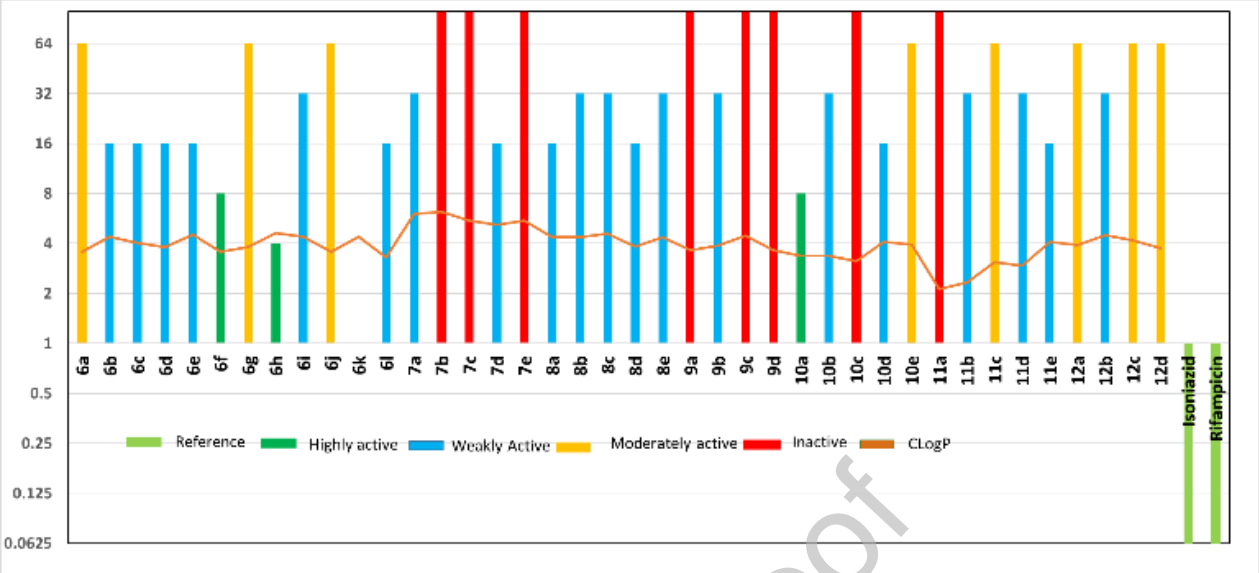

Figure 4: SAR inferences on isoxazoline carboxamide derivatives

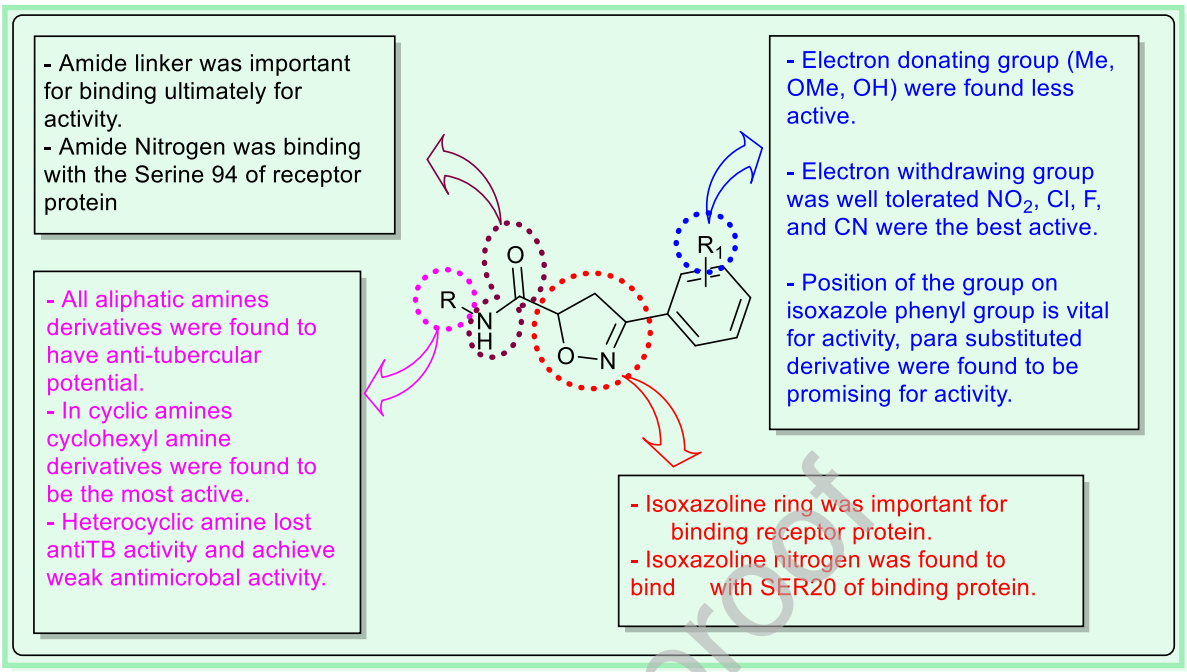

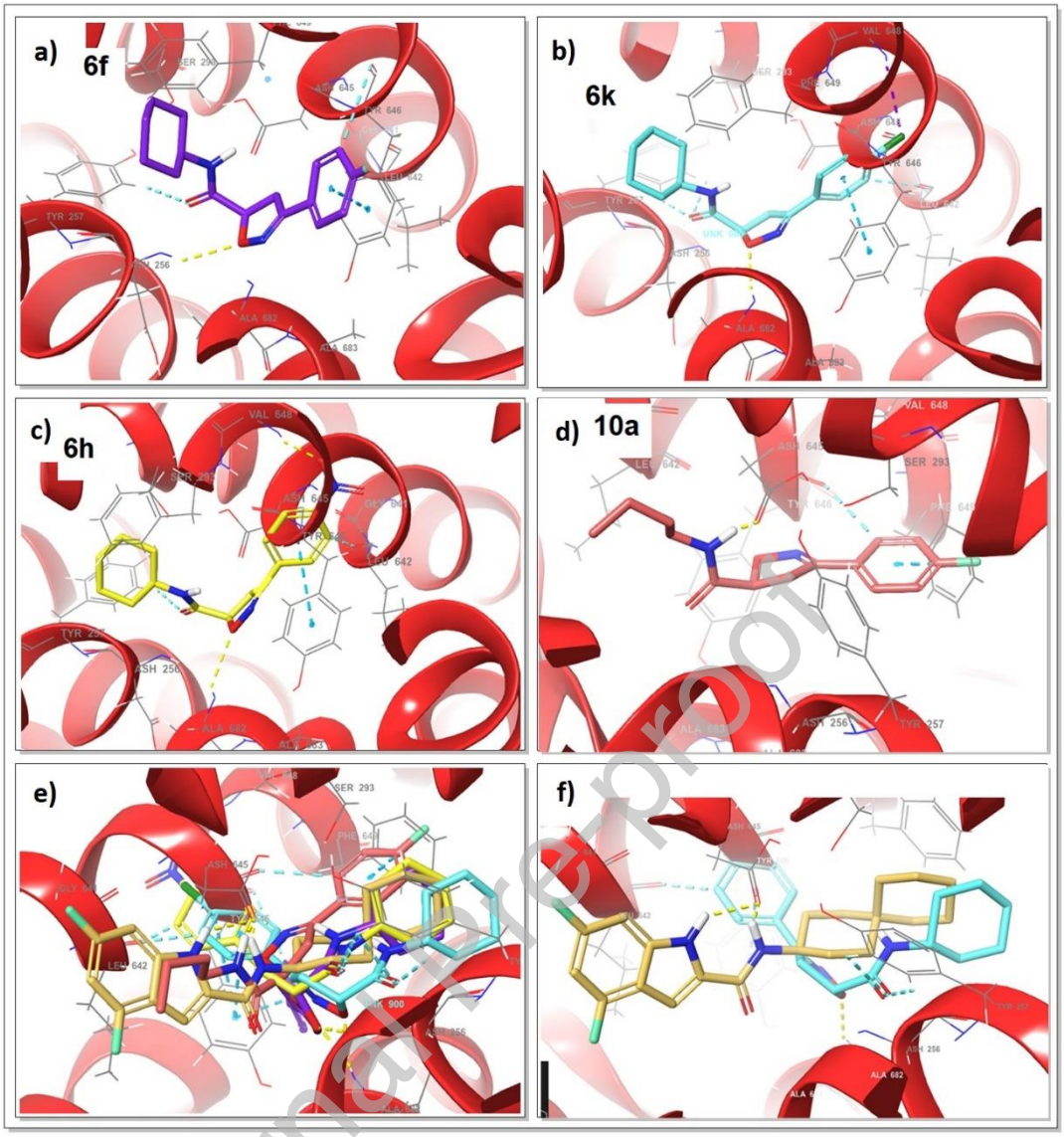

Figure 5: Ligand interactions between most active molecules and receptor protein. A) Compound **6f** (Purple) in the binding pocket of MmpL3 protein, exhibited π-π stacking interactions with TYR646. B) Compound **6k** (Sky-blue) in the binding pocket of MmpL3 protein. C) Compound **6h** (yellow) in the binding pocket of MmpL3 protein, exhibited π-π stacking interactions with TYR646. D) Compound **10a** (pink) in the displayed hydrogen bonding with ASH645. E) Compound **6f**, **6h**, **6k**, and **10a**, and co-crystal ligand in the binding pocket depicted a similar binding pattern of all active derivative except **10a** which bound inverted relative to others. F) Co-crystal ligand and compound **6k** superimposition show a similar binding pattern.

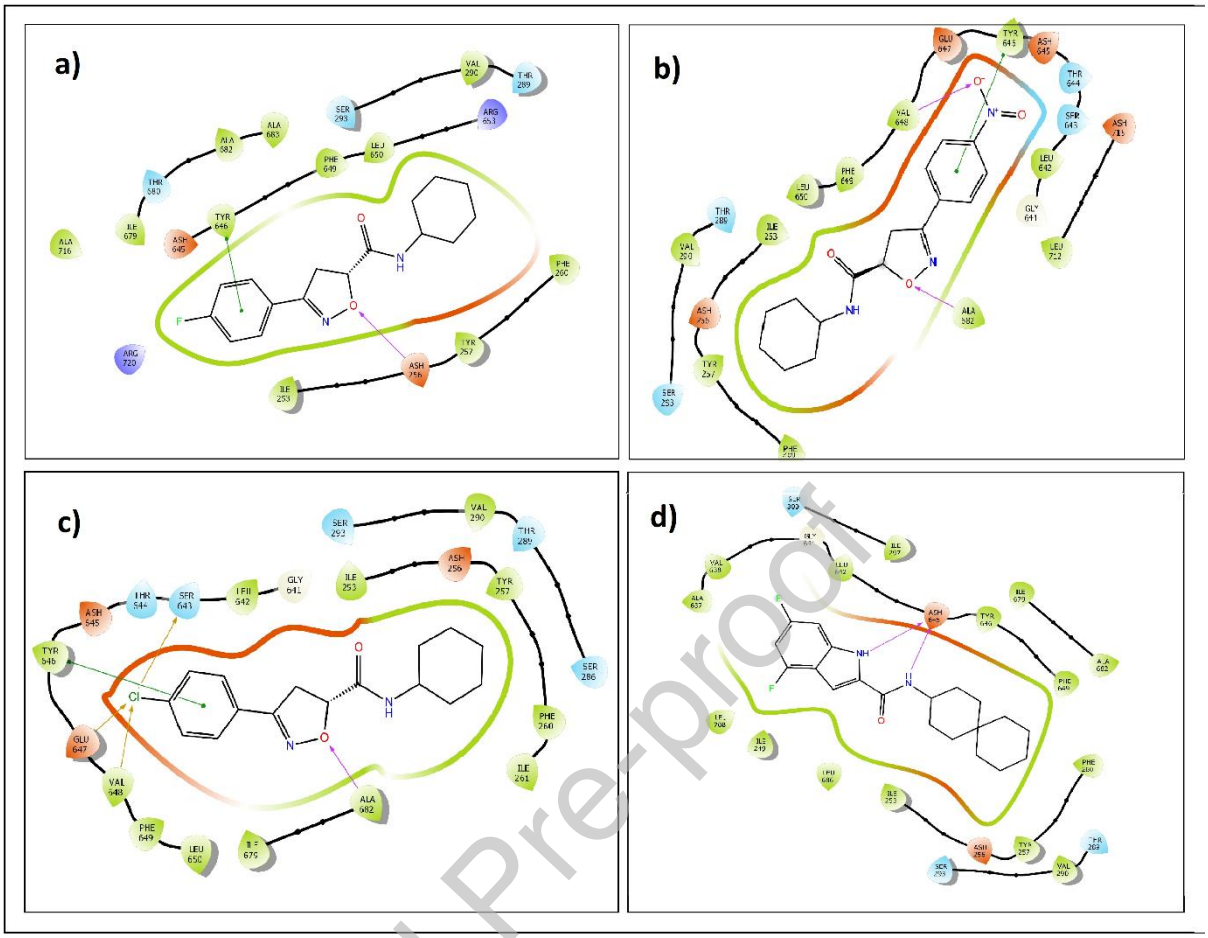

Figure 6: 2D Ligand interactions between most active molecules, co-crystal, and receptor protein (6AJJ). a) 2D Ligand interaction diagram representing compound **6f** in the binding pocket. b) Interactions diagram for the compound **6h** exhibited π-π stacking interactions with TYR646 shown by the green line. c) Representation of compound **6k** associated with multiple interactions as π-π stacking interactions with TYR646, hydrogen bonding with ALA682, and a yellow line representing the Halogen bond interactions. d) 2D representation of Co-crystal ligand observed to have hydrogen bond interactions with ASH645 denoted by the pink line.

Graphical abstract: